Manuscript ID: DTART092015003431

Electronic supporting information (ESI)

Dual mode ratiometric recognition of zinc acetate: nano-molar detection with *in-vitro* tracking of endophytic bacteria in rice root tissue

Abhijit Ghosh[a] , Sabyasachi Ta[a] , Milan Ghosh[a], Subhajit Karmakar[b], Avishek Banik[c], Tushar Kanti Dangar[c], Subhrakanti Mukherjee[d], and Debasis Das*[a]

[a]*Department of Chemistry, The University of Burdwan, Golapbag, Burdwan, India, Fax: +91-342-2530452; Tel: +91-342-2533913 (ext. 424); E-mail: ddas100in@yahoo.com*
[b]University Science Instrumentation Center, The University of Burdwan, Burdwan, West Bengal, India.
[c]Microbiology Laboratory, Crop production division, ICAR- Central Rice Research Institute. Cuttack, Odisha, India.
[d]Department of Microbiology, The University of Burdwan, Burdwan, West Bengal, India.

Calculations of detection limit: The values for $\frac{I_x - I_0}{I_{max} - I_0}$ from the respective fluorescence titration graphs are plotted against the concentration of ZA and the points of concentration axex at which the best linear fitted line crosses are taken as the detection limits.

Now, for A4; I_{max} = 1263 I_0 = 233, (I_{max} − I_0) = 1030

Conc. of ZA (μM)	I_x	(I_x – I_0)	(I_x – I_0)/(I_{max} − I_0)
0.05	249	16	0.01553
0.1	267	34	0.03301
0.2	290	57	0.05534
0.3	328	195	0.09223
0.4	373	140	0.13592
0.6	418	185	0.17961
0.7	463	230	0.2233
0.8	493	260	0.25243

Now, plot of $\frac{I_x - I_0}{I_{max} - I_0}$ vs. [ZA] based on Y = A+ B*X (A = -0.00095, B = 0.31580, R = 0.99767) crosses the concentration axis at 0.003 μM, i.e., at 3.0 nM, which is considered to be the detection limit for ZA using A4.

Similarly, for A5; I_{max} = 1113, I_0 = 13, (I_{max} − I_0) = 1100

Conc. of ZA (μM)	I_x	(I_x – I_0)	(I_x – I_0)/(I_{max} − I_0)
0.05	33	20	0.01818

0.1	63	50	0.04545
0.2	83	70	0.06364
0.3	113	100	0.09091
0.4	173	160	0.14545
0.6	223	210	0.19091
0.7	283	270	0.24545
0.8	343	330	0.3

Now, plot of $\frac{I_x - I_0}{I_{max} - I_0}$ vs. [ZA] based on Y = A+ B*X (A = -0.00289, B = 0.35654, R = 0.99213) crosses the concentration axis at 0.0081 µM, i.e., at 8.1 nM, which is considered to be the detection limit for ZA using A5.

Also for A6; I_{max} = 1145 I_0 = 145, (I_{max} − I_0) = 1000

Conc. of ZA (µM)	I_x	(I_x – I_0)	(I_x – I_0)/(I_{max} − I_0)
0.3	285	140	0.14
0.4	315	170	0.17
0.5	375	230	0.23
0.6	435	290	0.29
0.7	465	320	0.32
0.9	555	410	0.41

Now, plot of $\frac{I_x - I_0}{I_{max} - I_0}$ vs. [ZA] based on Y = A+ B*X (A = -0.00229, B = 0.46286, R = 0.99591) crosses the concentration axis at 0.0049 µM, i.e., at 4.9 nM, which is considered to be the detection limit for ZA using A6.

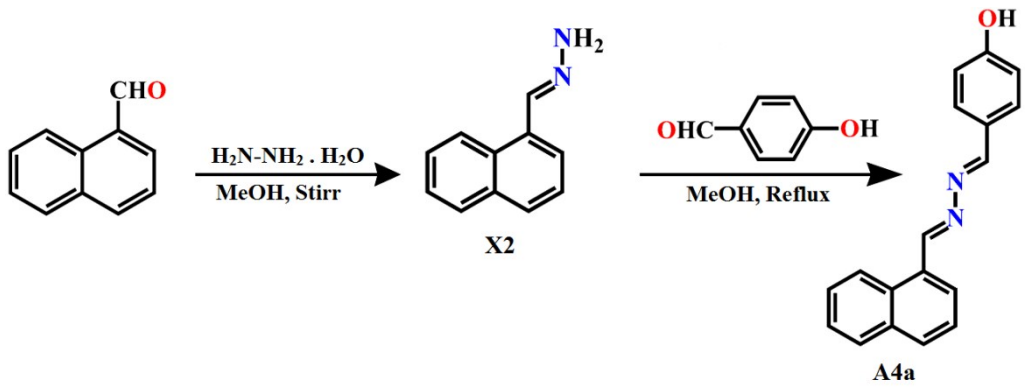

Scheme S1

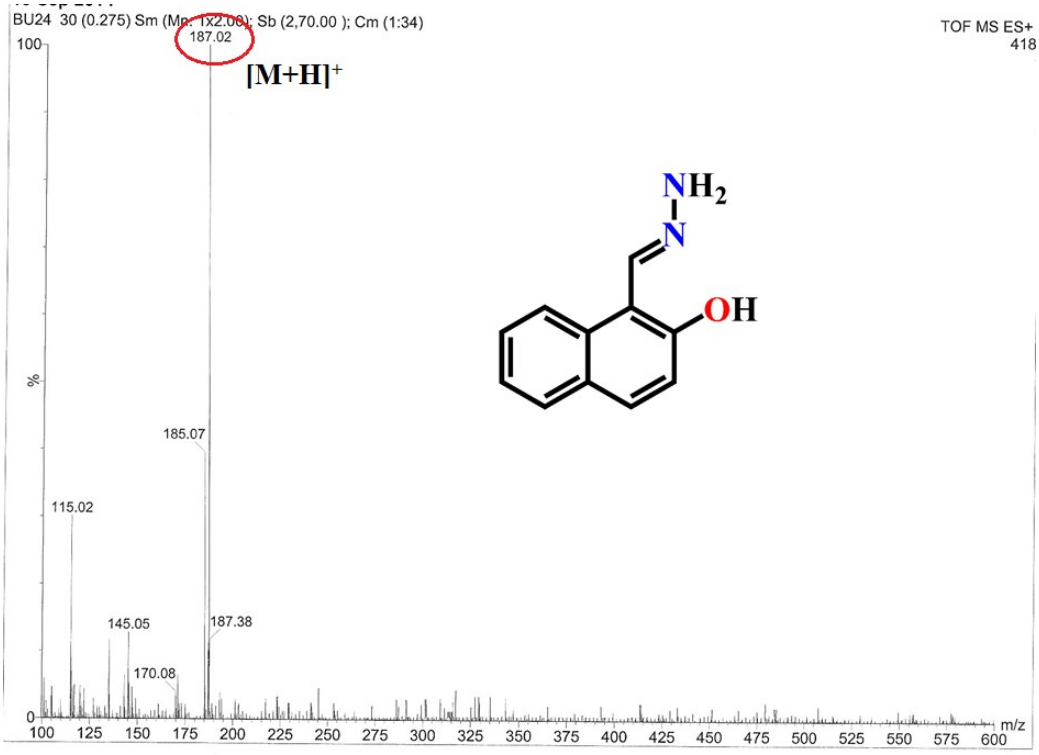

Fig. S1 Mass spectrum of X1

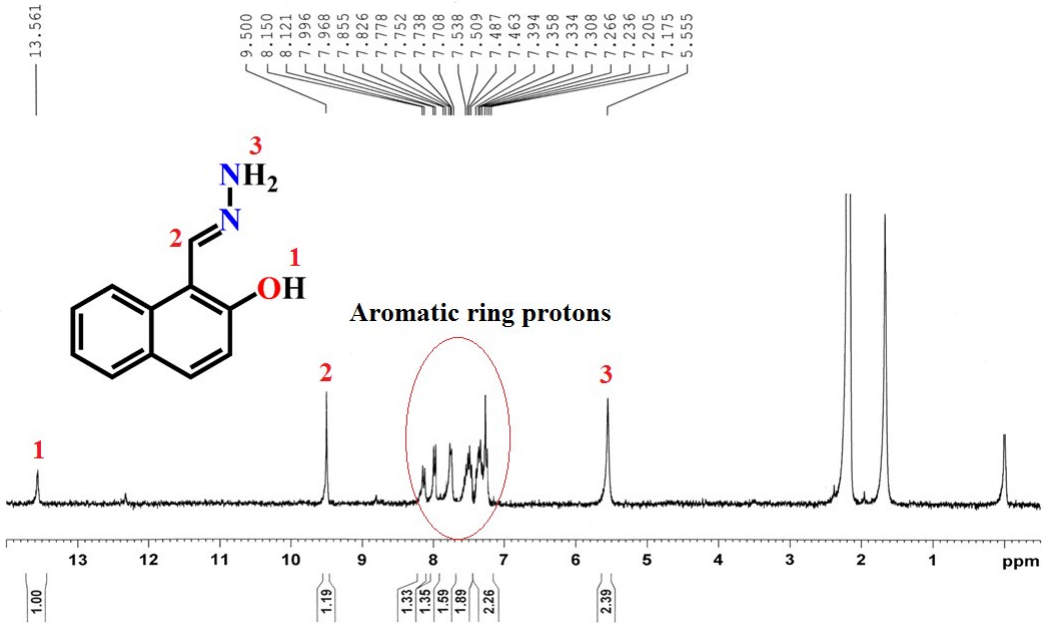

Fig. S2 ^{1}H NMR spectrum of X1 in $CDCl_3$

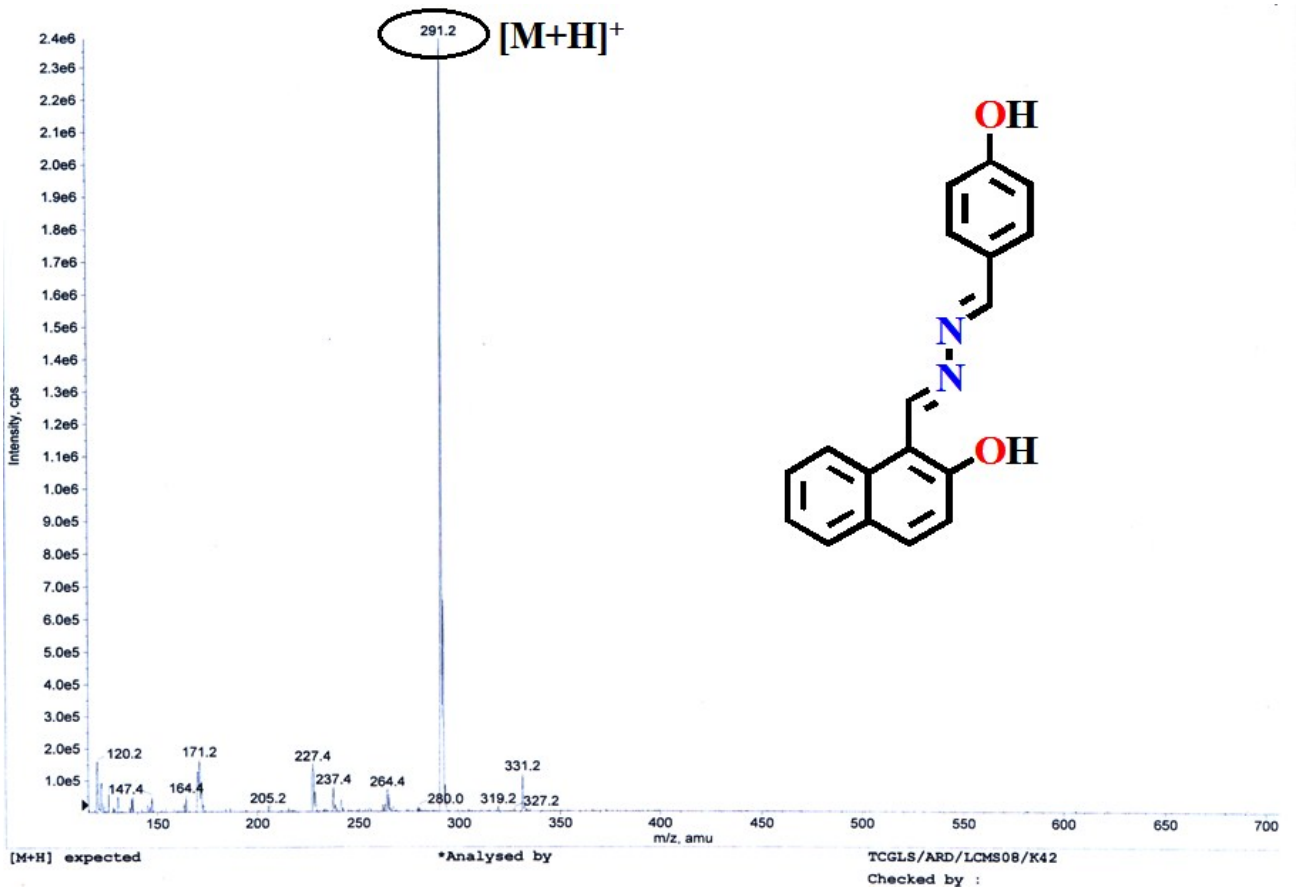

Fig. S3 Mass spectrum of A4

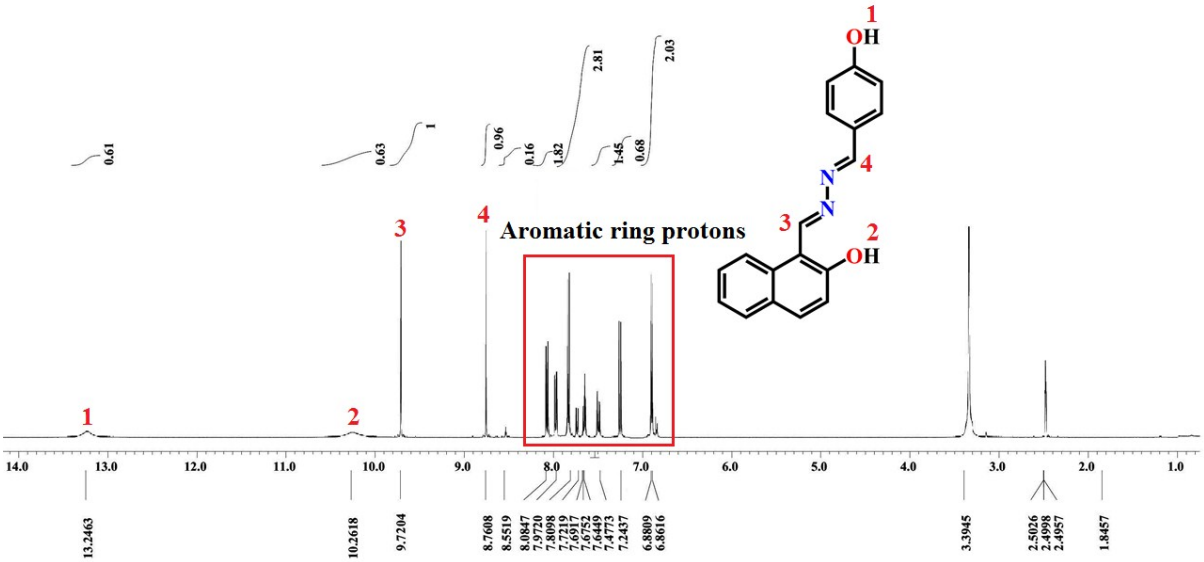

Fig. S4 ^{1}H NMR spectrum of A4 in DMSO-d_6

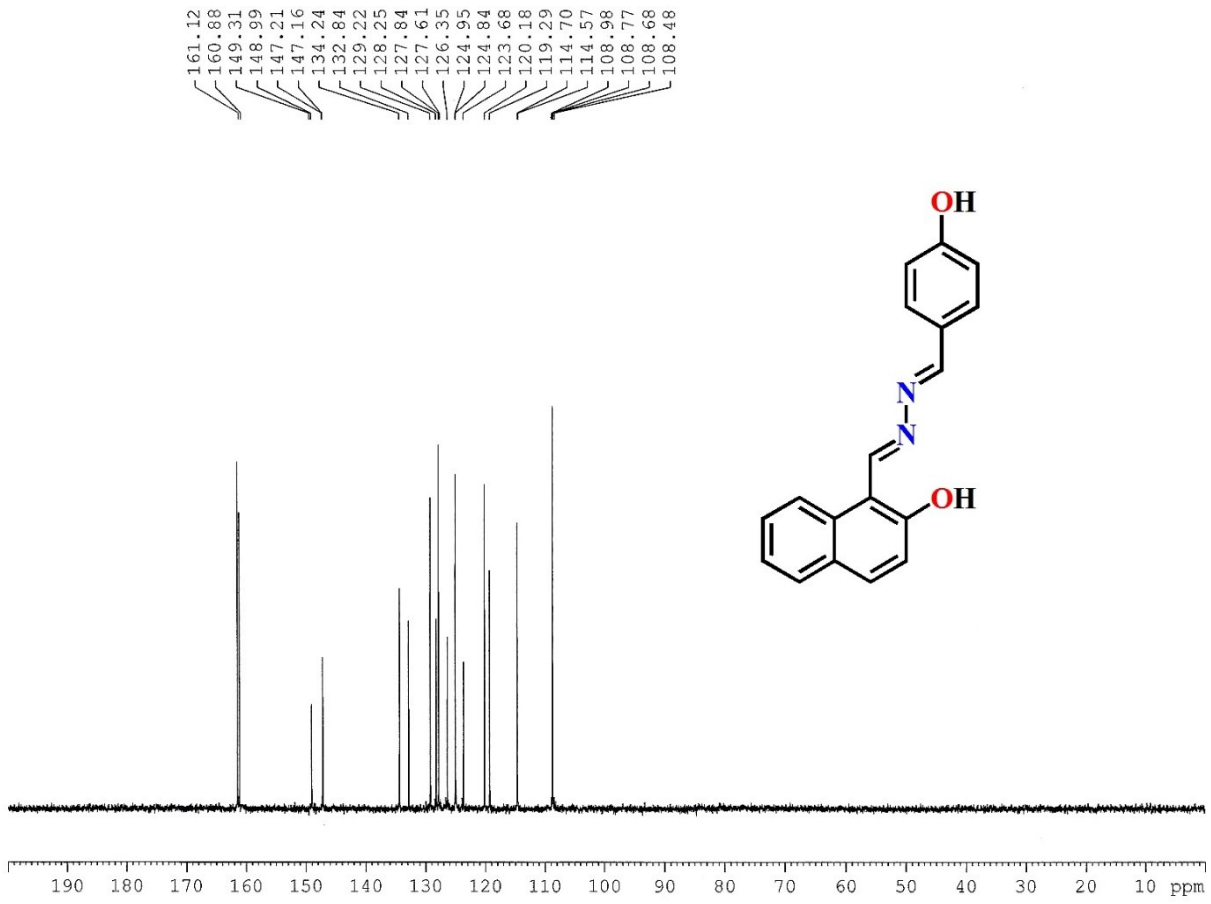

Fig. S5 ^{13}C NMR spectrum of A4 in $CDCl_3$

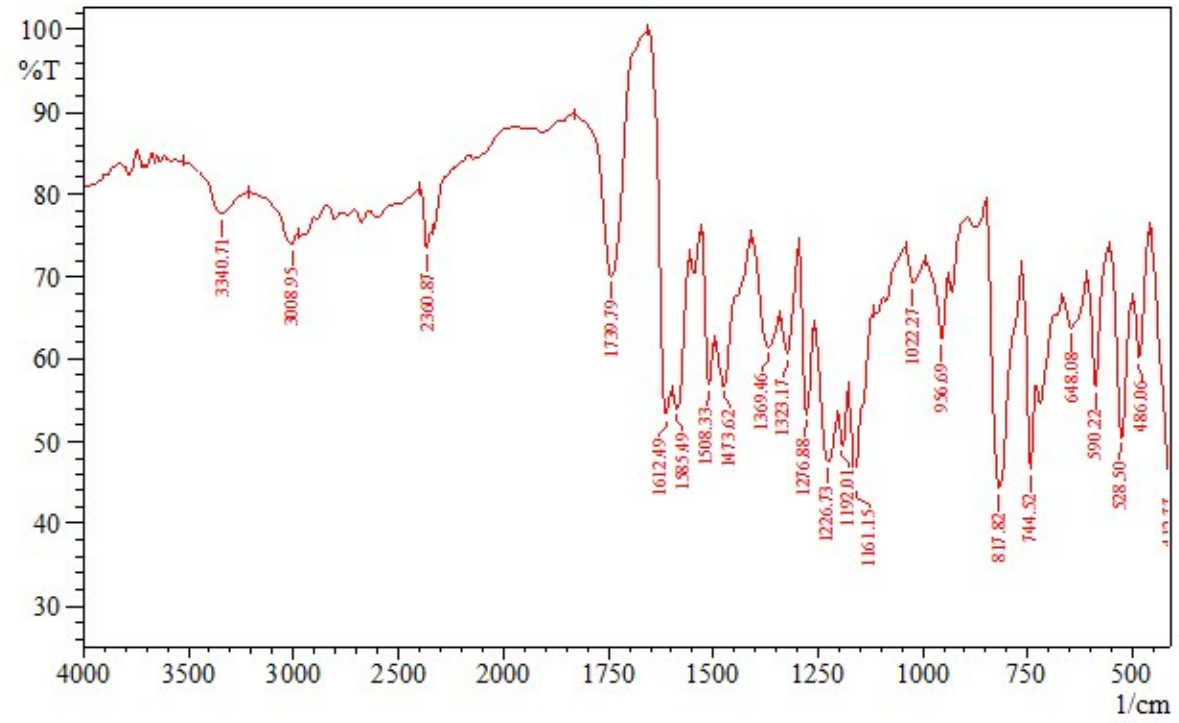

Fig. S6 FTIR spectrum of A4

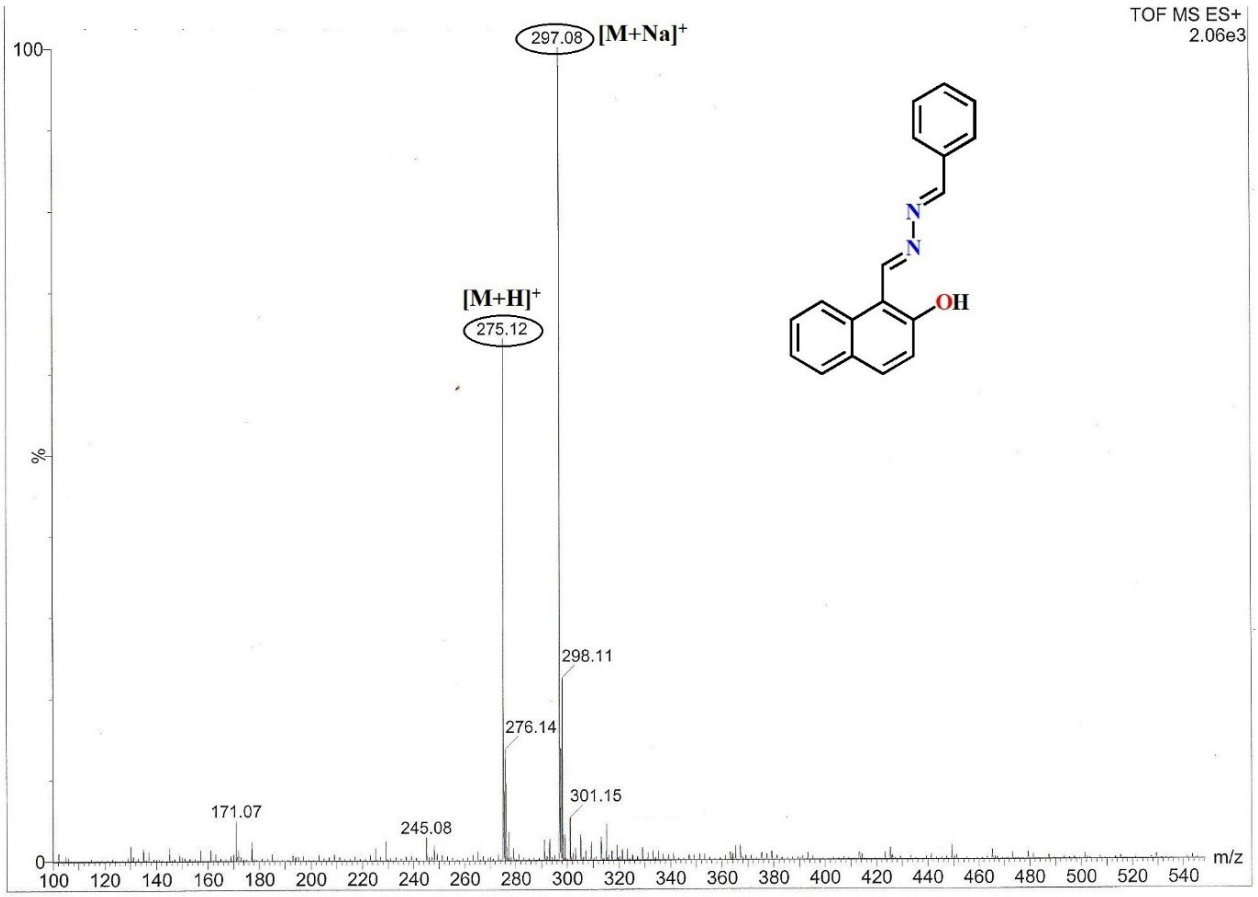

Fig. S7 Mass spectrum of A5

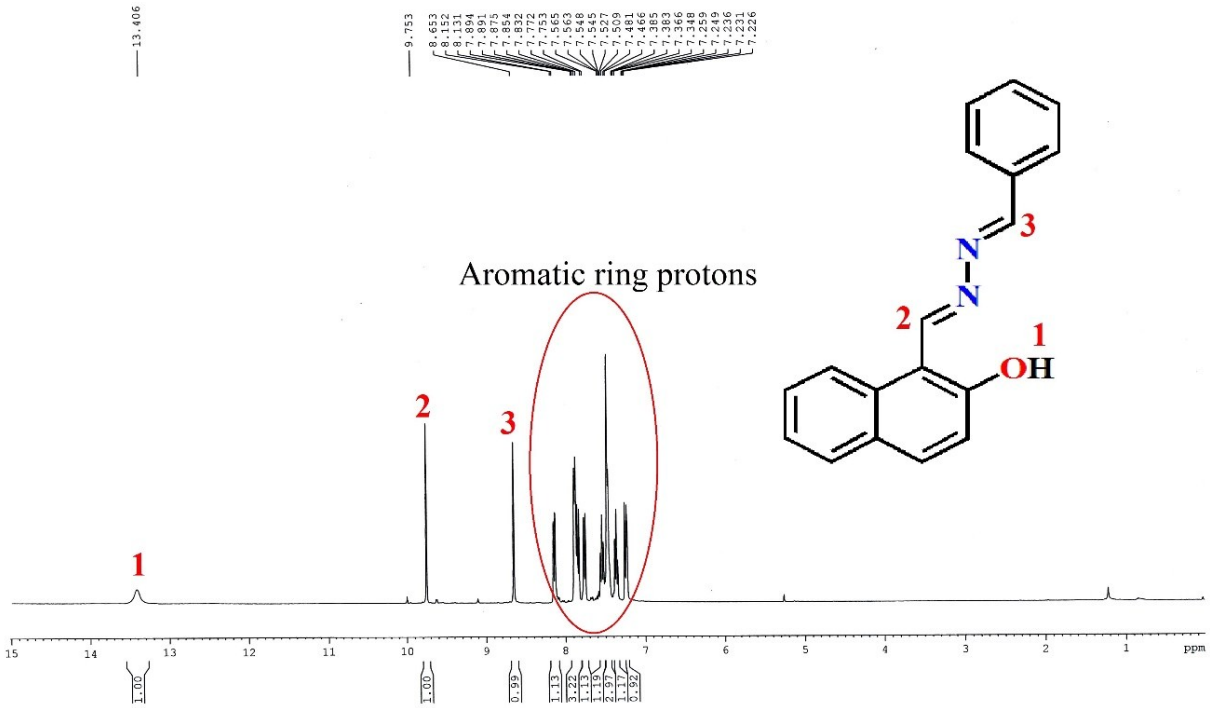

Fig. S8 ^{1}H NMR spectrum of A5 in $CDCl_3$

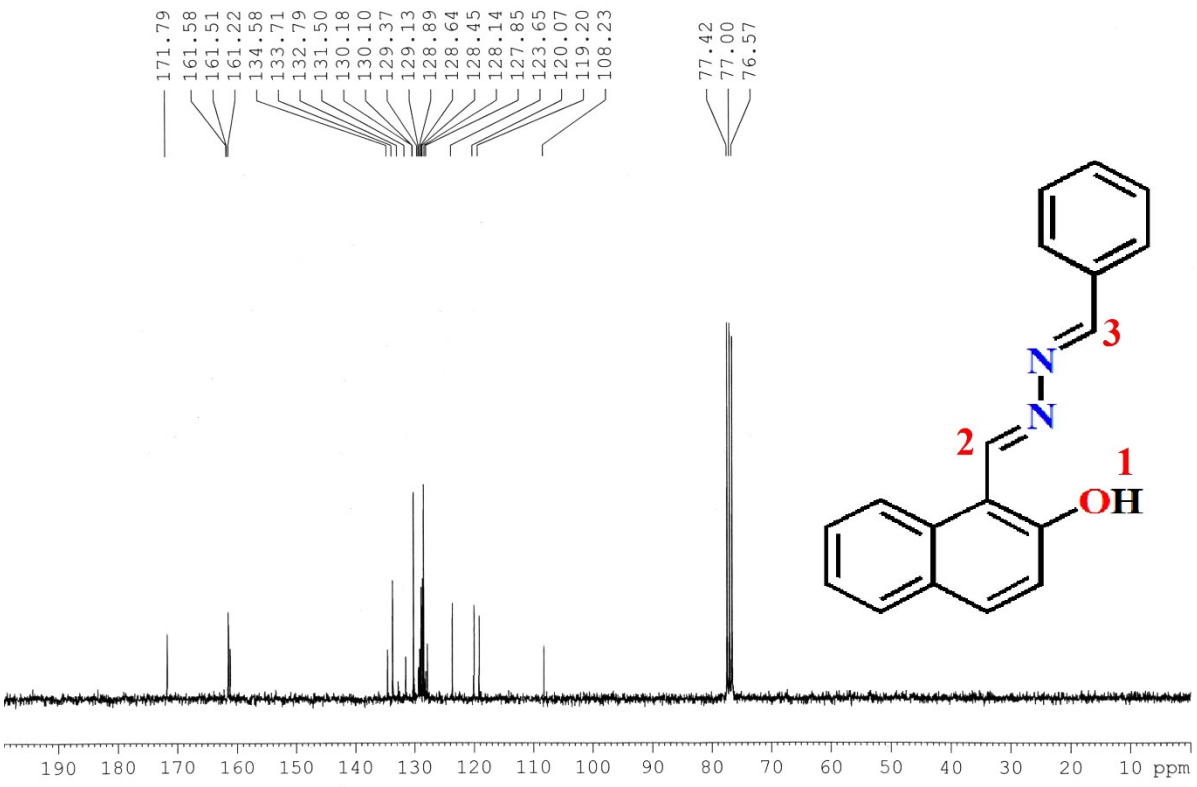

Fig. S9 ^{13}C NMR spectrum of A5 in $CDCl_3$

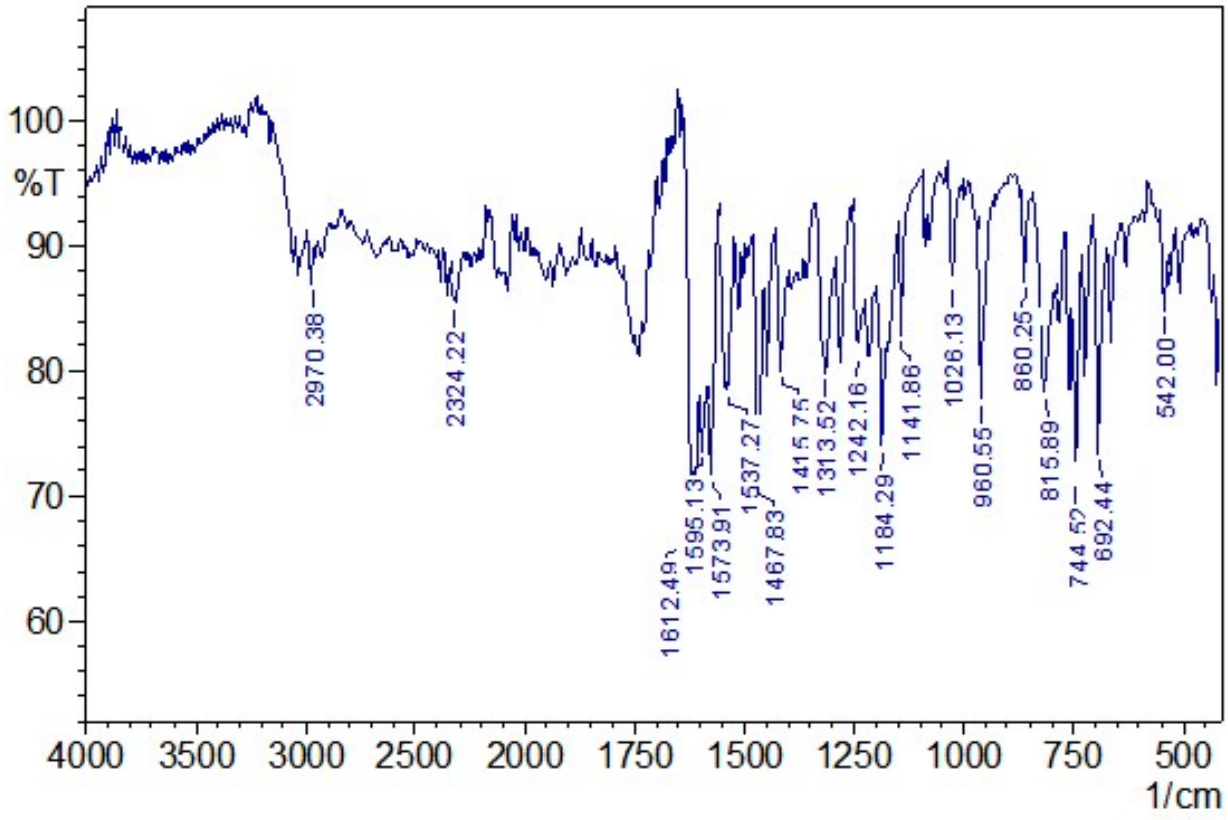

Fig. S10 FTIR spectrum of A5

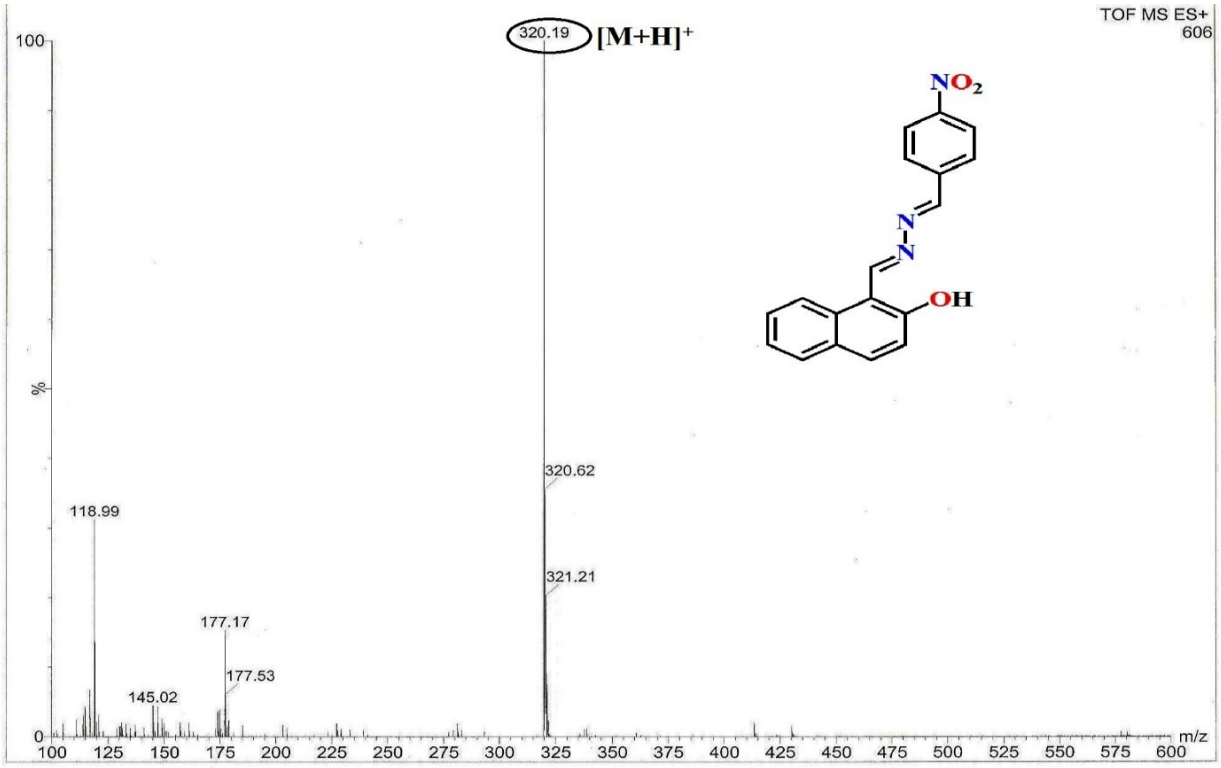

Fig. S11 Mass spectrum of A6

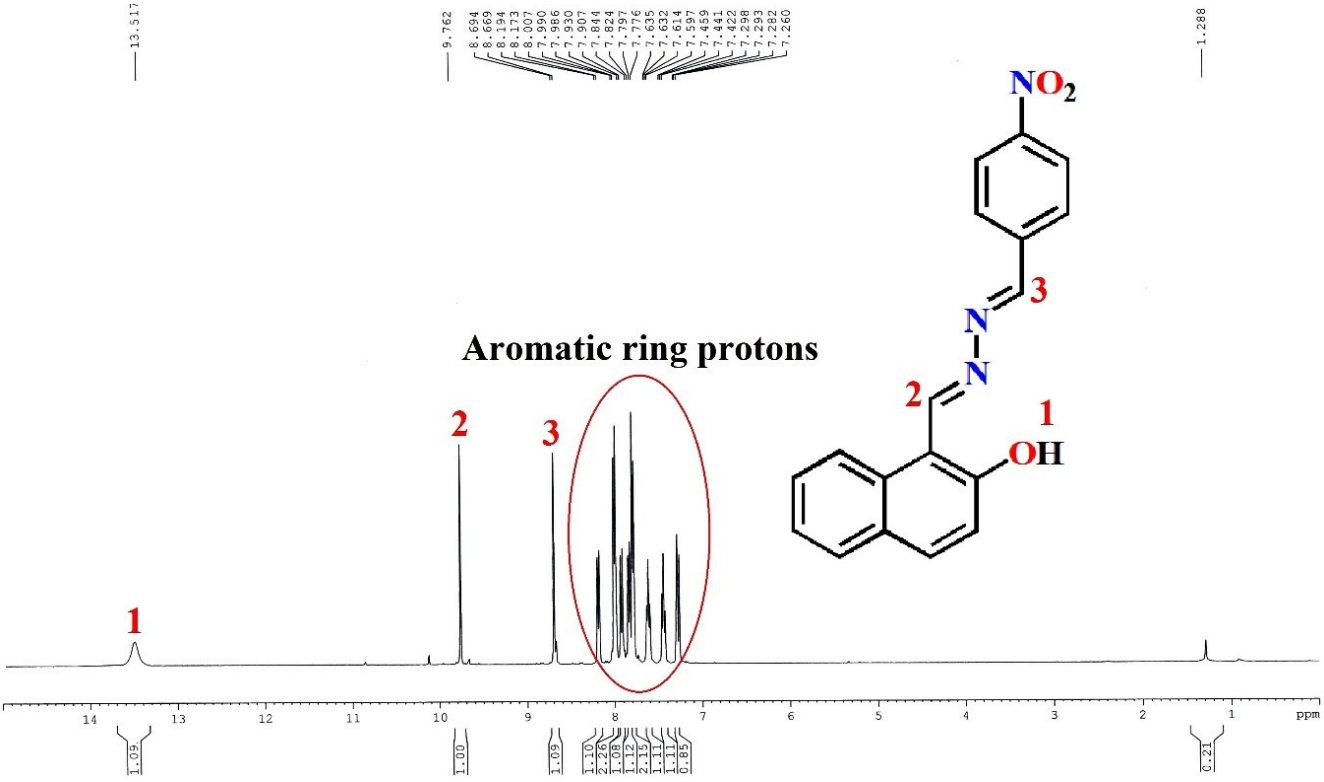

Fig. S12 ^{1}H NMR spectrum of A6 in $CDCl_3$

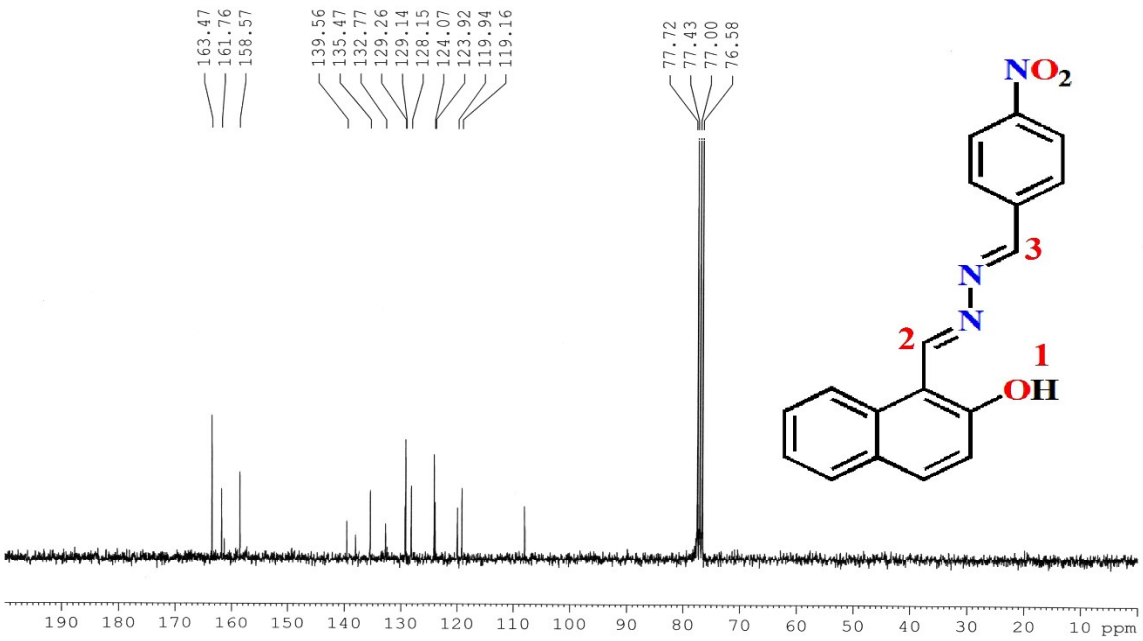

Fig. S13 ^{13}C NMR spectrum of A6 in $CDCl_3$

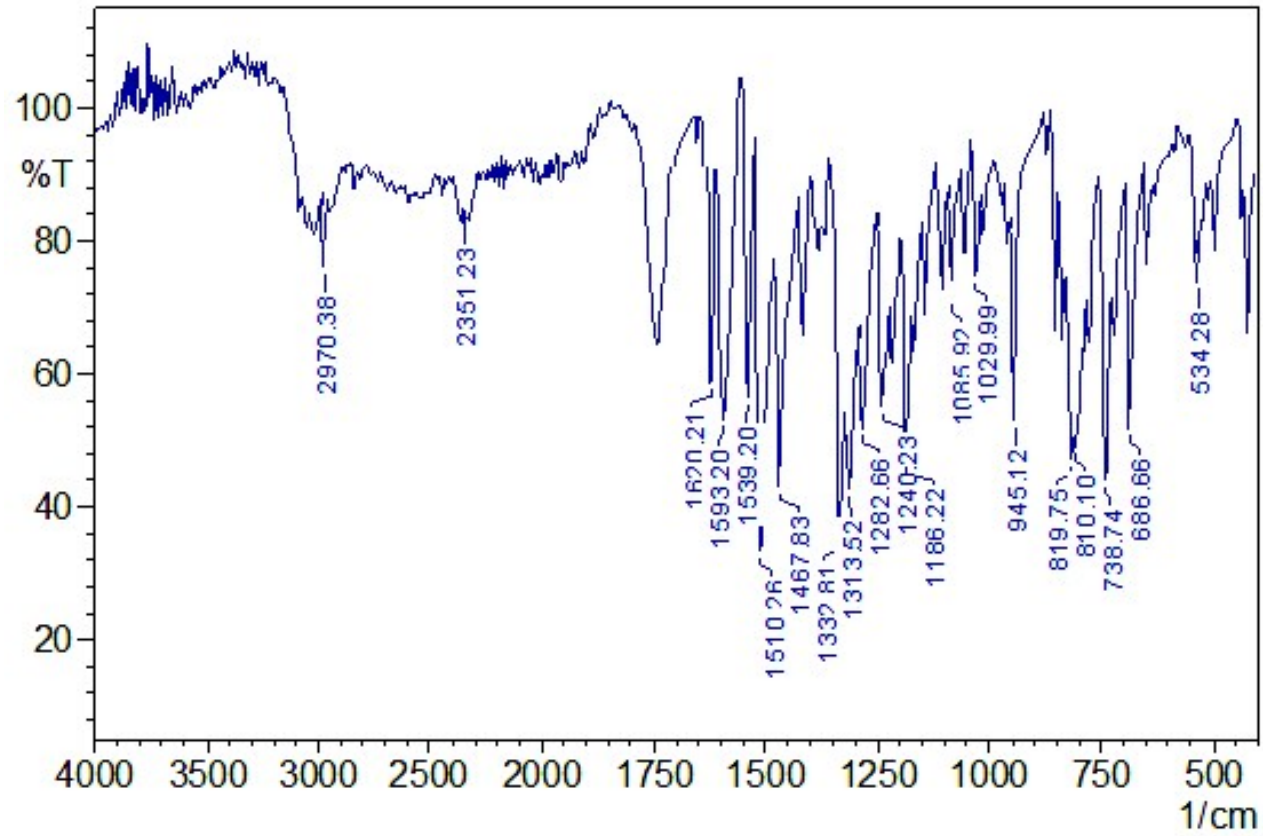

Fig. S14 FTIR spectrum of A6

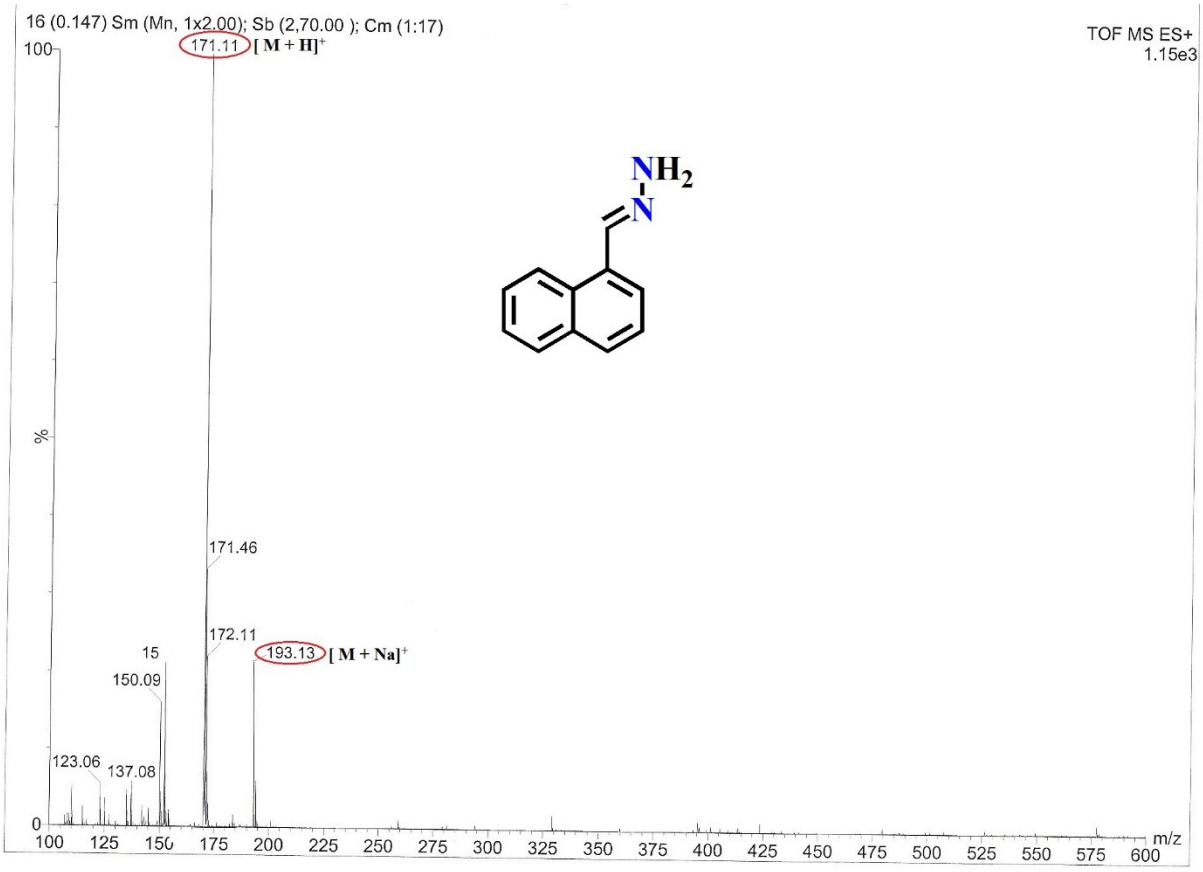

Fig. S15 Mass spectrum of X2

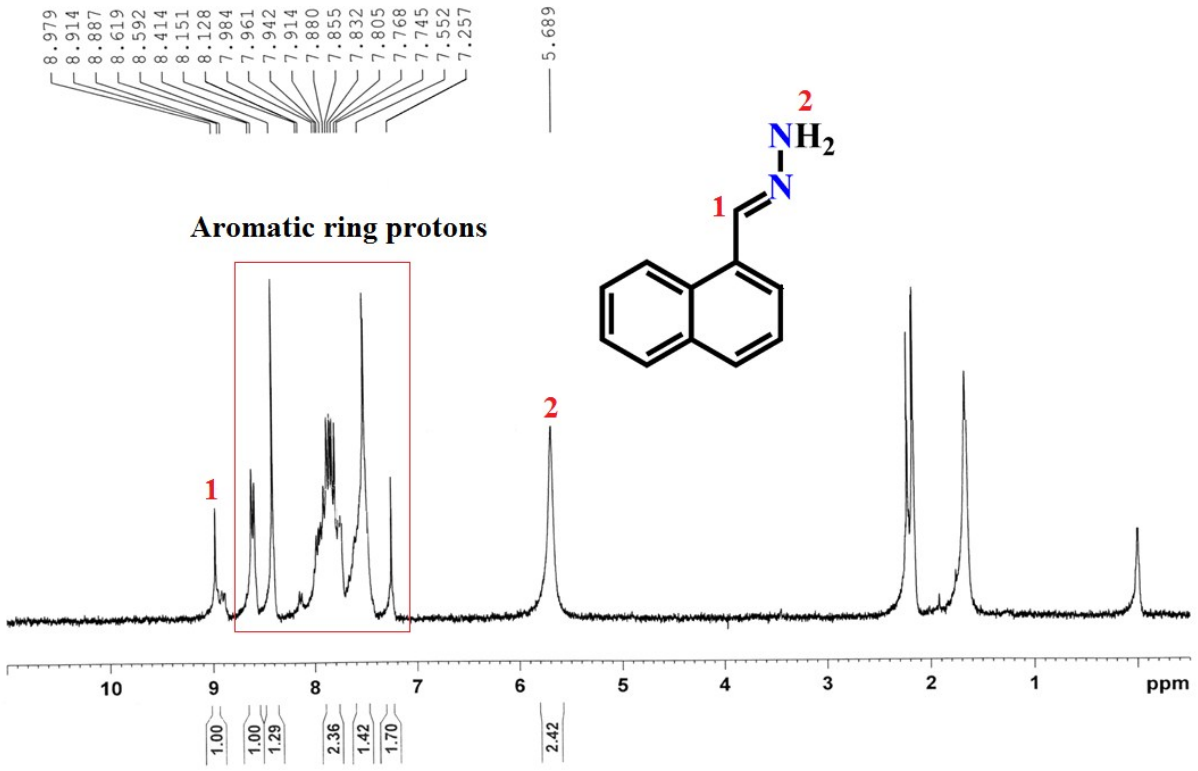

Fig. S16 ^{1}H NMR spectrum of X2 in $CDCl_3$

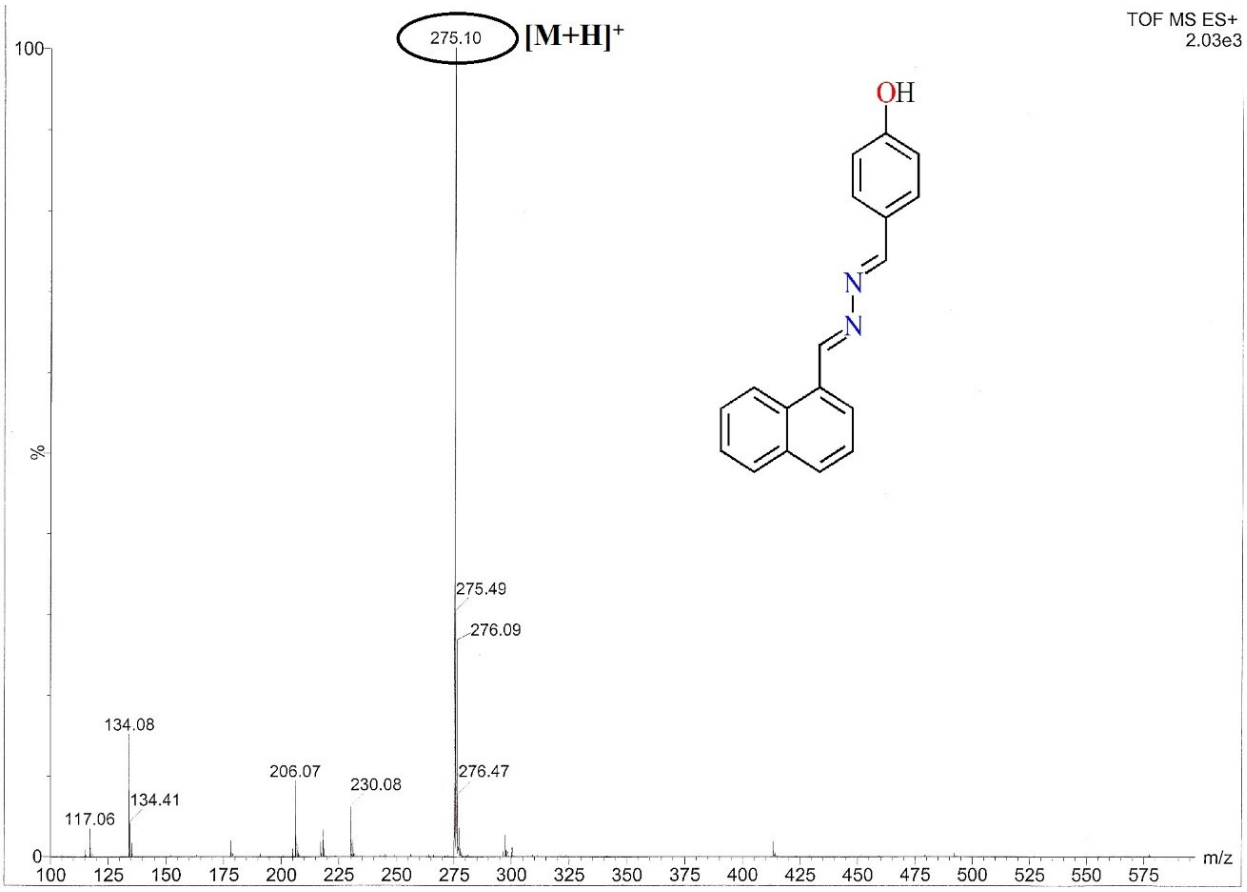

Fig. S17 Mass spectrum of A4a

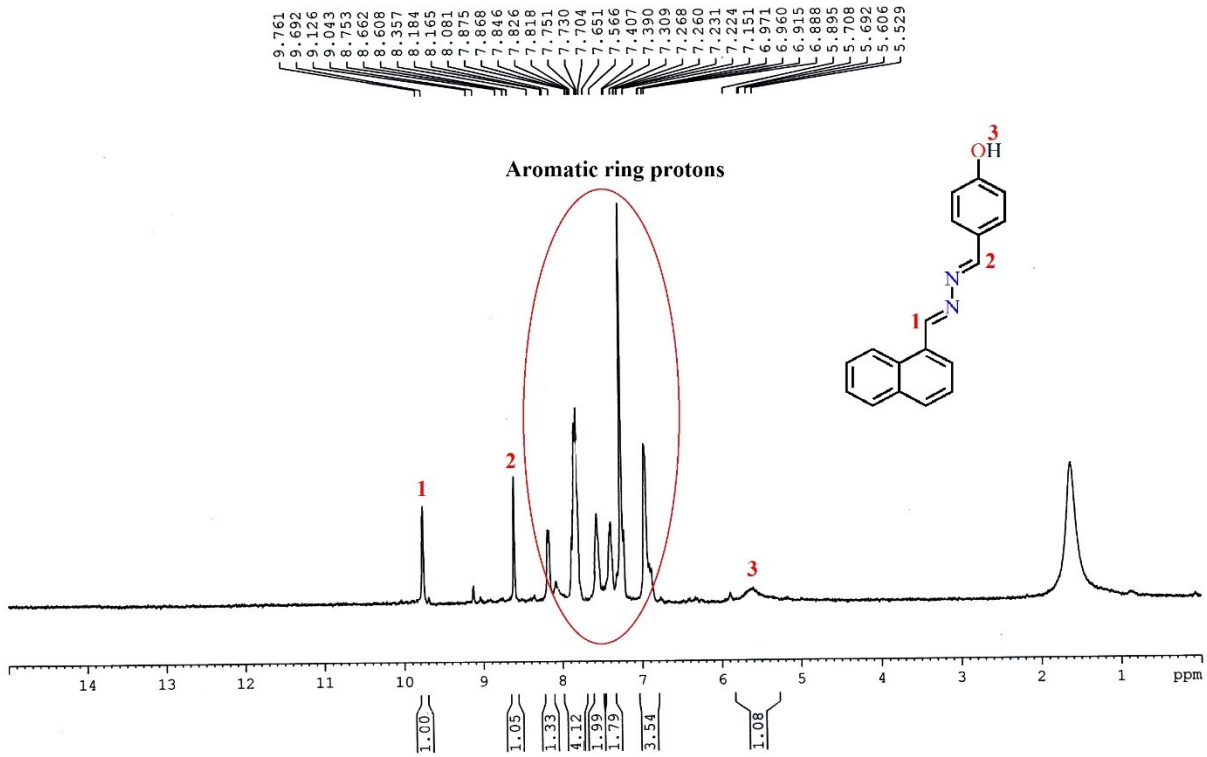

Fig. S18 ^{1}H NMR spectrum of A4a in $CDCl_3$

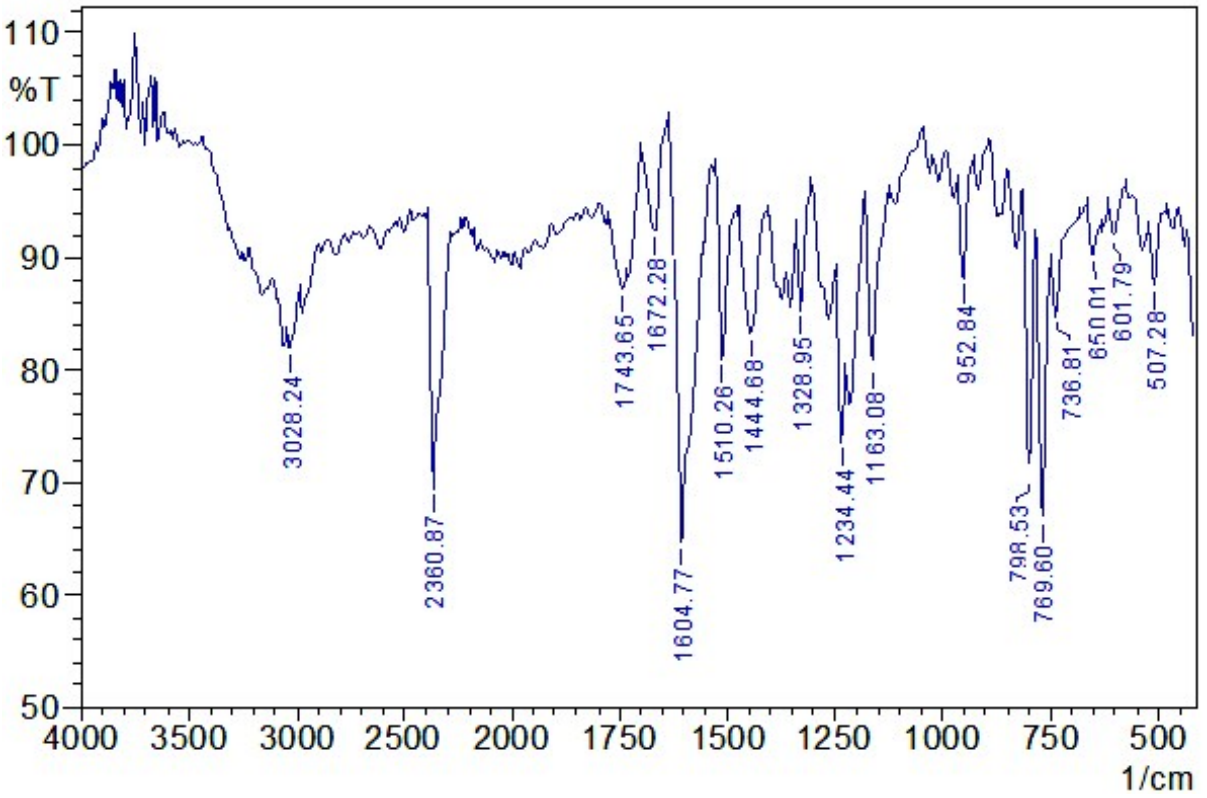

Fig. S19 FTIR spectrum of A4a

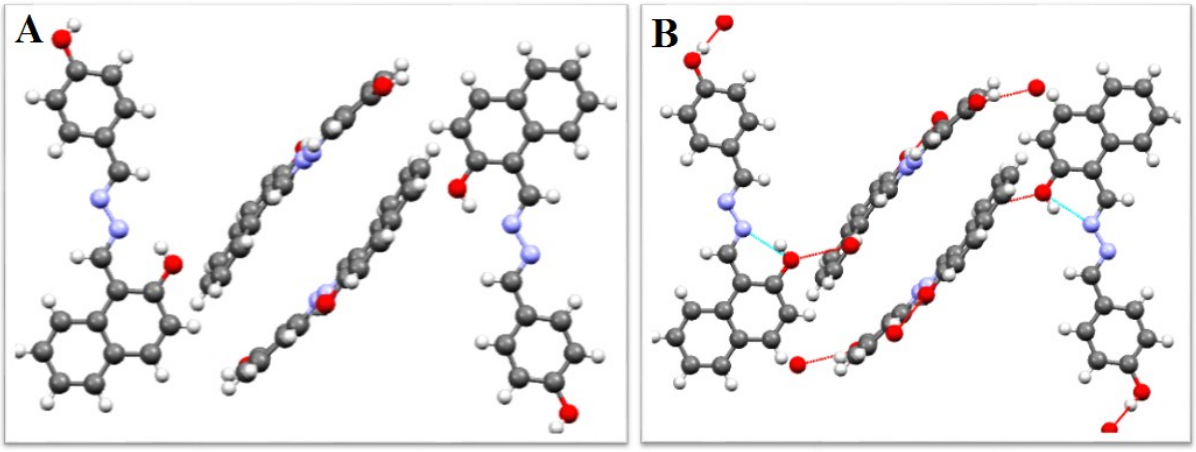

Fig. S20 (A) Crystal packing and (B) H-bonding network of A4

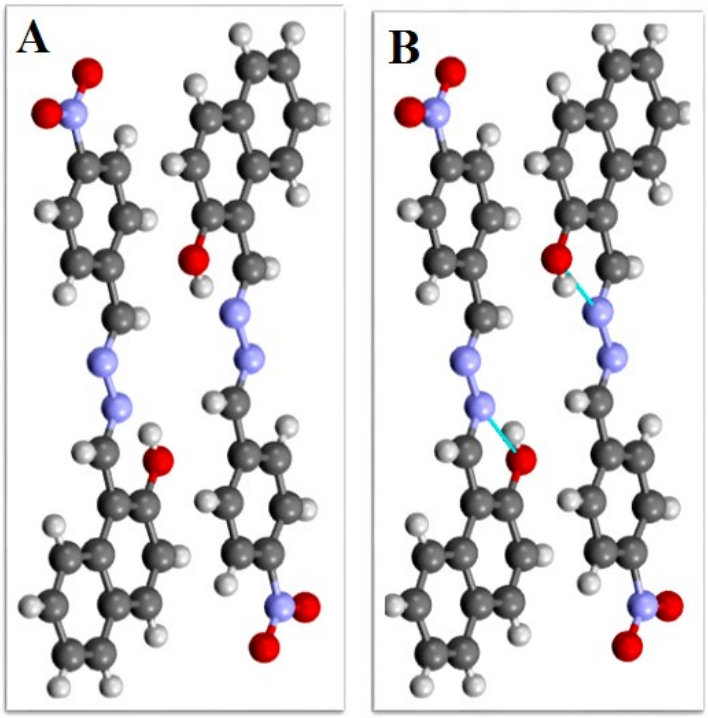

Fig. S21 (A) Crystal packing and (B) H-bonding network of A6

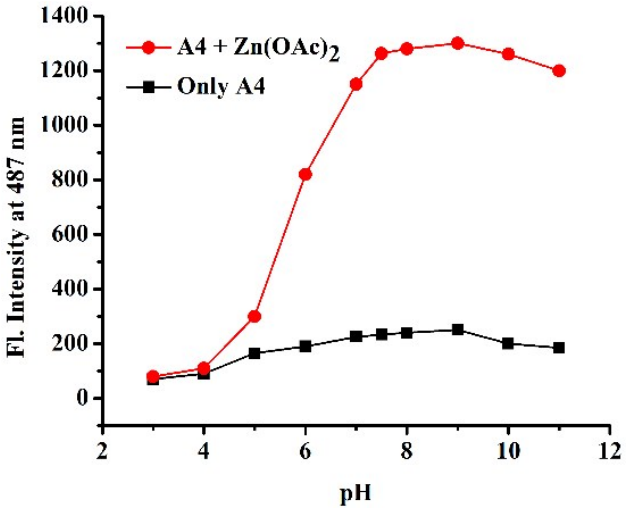

Fig. S22 Effect of pH on the emission intensities of **A4** (10 μM) before and after addition of $Zn(OAc)_2$ (400 equiv.), λ_{ex} = 370 nm; λ_{em} = 487 nm

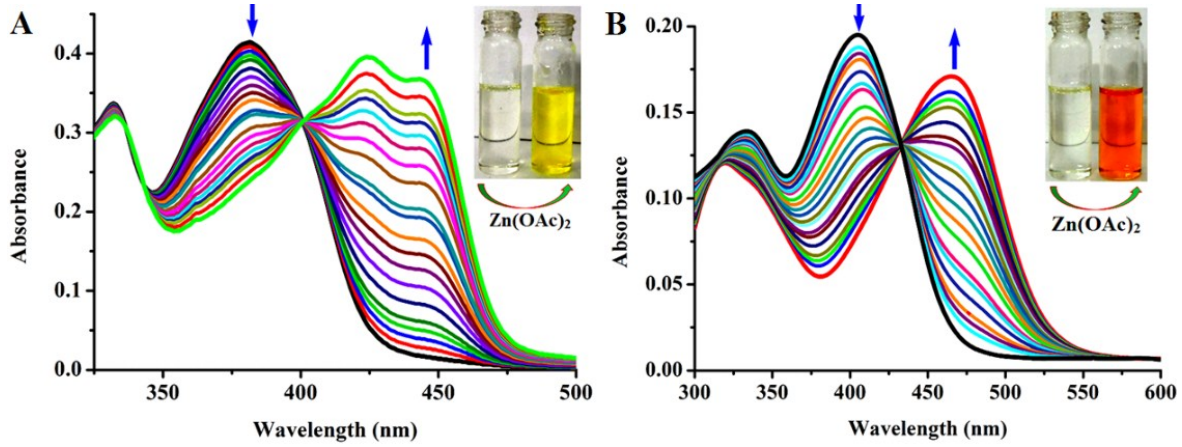

Fig. S23 Changes in the absorption spectra of [A] A5 (10 μM) and [B] A6 (10 μM) (DMSO– water (9: 1, v/v, 0.1 M HEPES buffer, pH 7.4) upon gradual addition of $Zn(OAc)_2$ (0-300 μM). Inset: the naked eye view of A5 and A6 before and after addition of $Zn(OAc)_2$

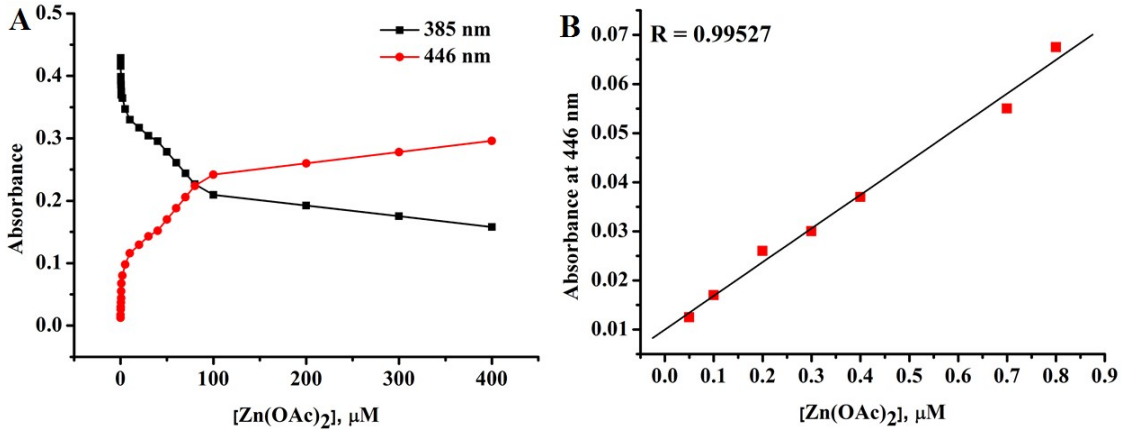

Fig. S24 Absorbance of **A4** (10 μM, DMSO– water (9: 1, v/v, 0.1 M HEPES buffer, pH 7.4) as a function of added $Zn(OAc)_2$ (0- 400 μM). Linear region of the plot (at 446 nm) (right)

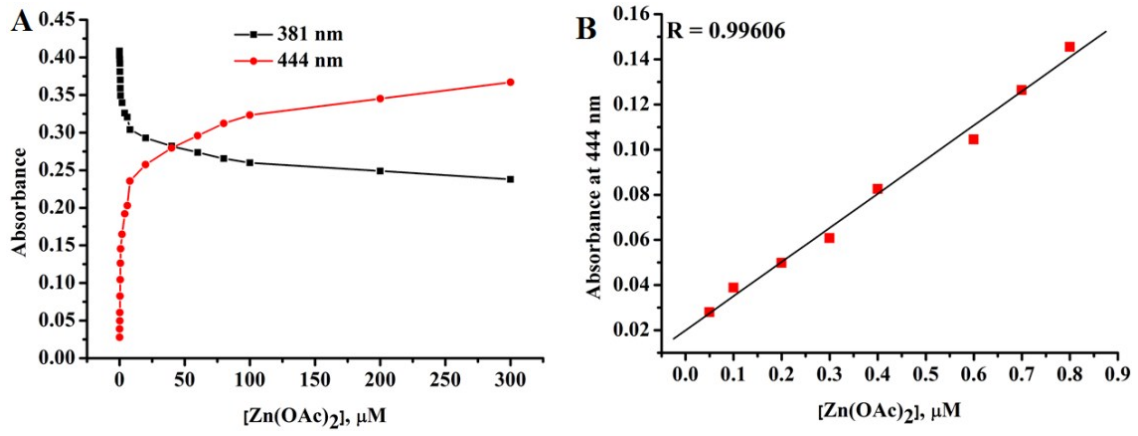

Fig. S25 Absorbance of **A5** (10 μM, DMSO– water (9: 1, v/v, 0.1 M HEPES buffer, pH 7.4) as a function of added $Zn(OAc)_2$ (0- 300 μM). Linear region of the plot (at 444 nm) (right)

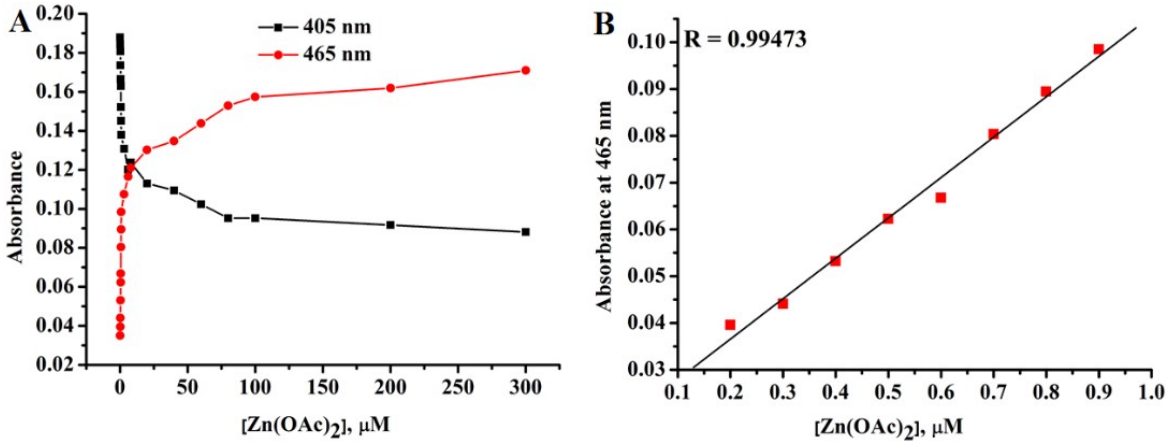

Fig. S26 Absorbance of **A6** (10 μM, DMSO– water (9: 1, v/v, 0.1 M HEPES buffer, pH 7.4) as a function of added $Zn(OAc)_2$ (0- 300 μM). Linear region of the plot (at 465 nm) (right)

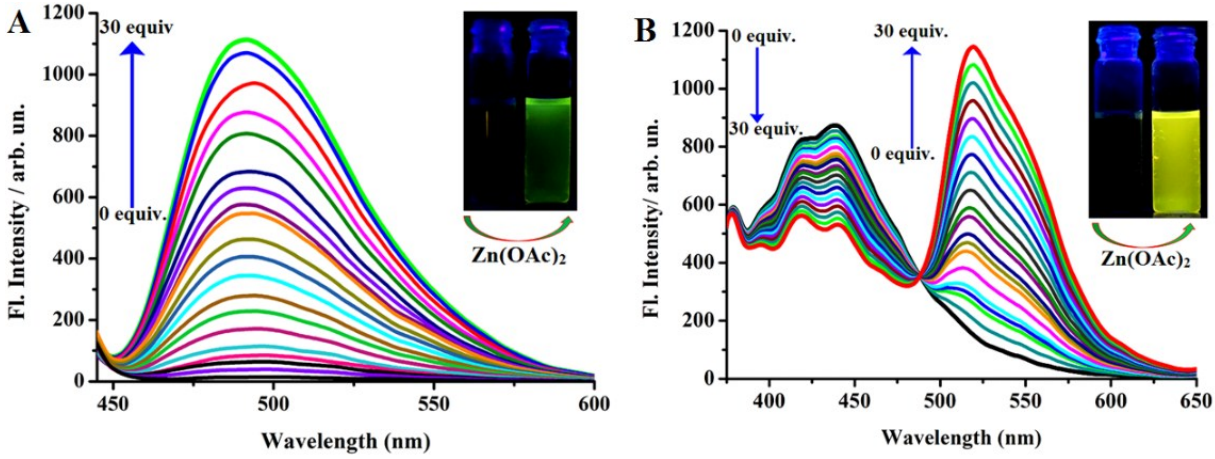

Fig. S27 Changes in the emission spectra of [A] A5 (10 μM , λ_{ex} 430 nm, λ_{em} 495 nm) and [B] A6 (10 μM , λ_{ex} 337 nm, λ_{em} 520 nm) (DMSO– water (9 : 1, v/v, 0.1 M HEPES buffer, pH 7.4) upon gradual addition of $Zn(OAc)_2$ (0-300 μM). Inset: UV light exposed colors of A5 and A6 before and after addition of $Zn(OAc)_2$

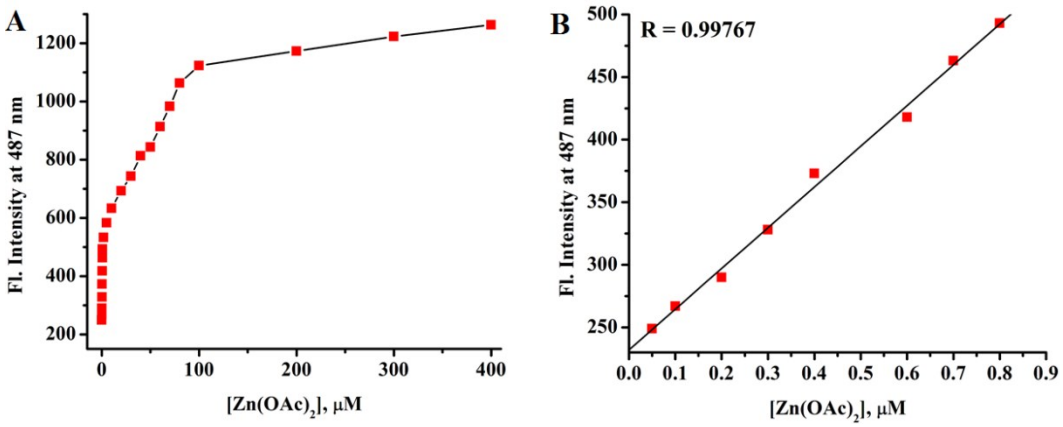

Fig. S28 Emission intensities of **A4** (10 µM, DMSO–water (9: 1, v/v, 0.1 M HEPES buffer, pH 7.4, λ_{ex}, 370 nm; λ_{em}, 487 nm) as a function of added $Zn(OAc)_2$ (0- 400 µM). Linear region of the plot (right)

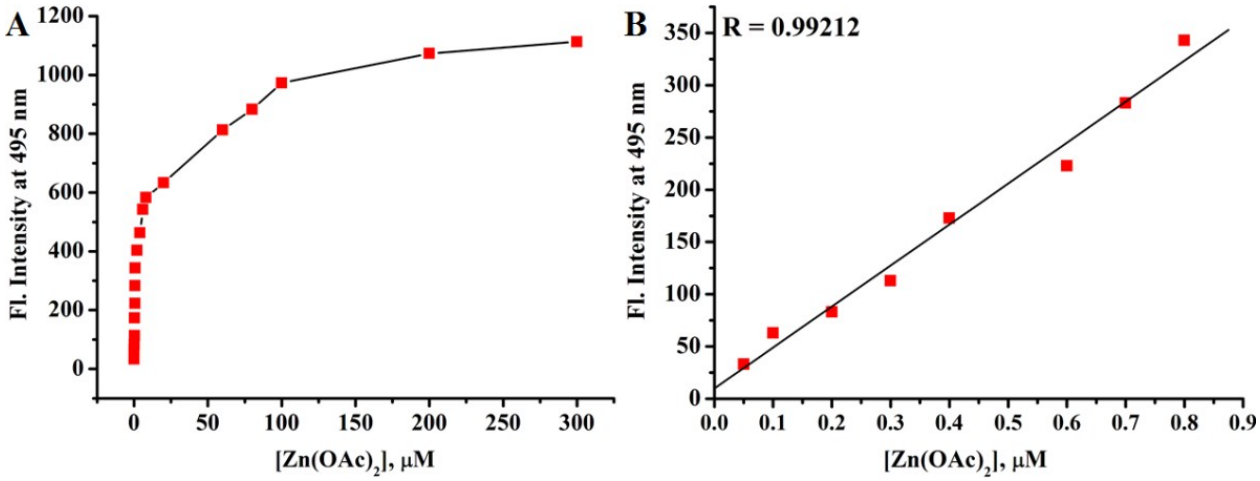

Fig. S29 Emission intensities of **A5** (10 µM, DMSO– water (9 : 1, v/v, 0.1 M HEPES buffer, pH 7.4, λ_{ex}, 430 nm; λ_{em}, 495 nm) as a function of added $Zn(OAc)_2$ (0- 300 µM). Linear region of the (right)

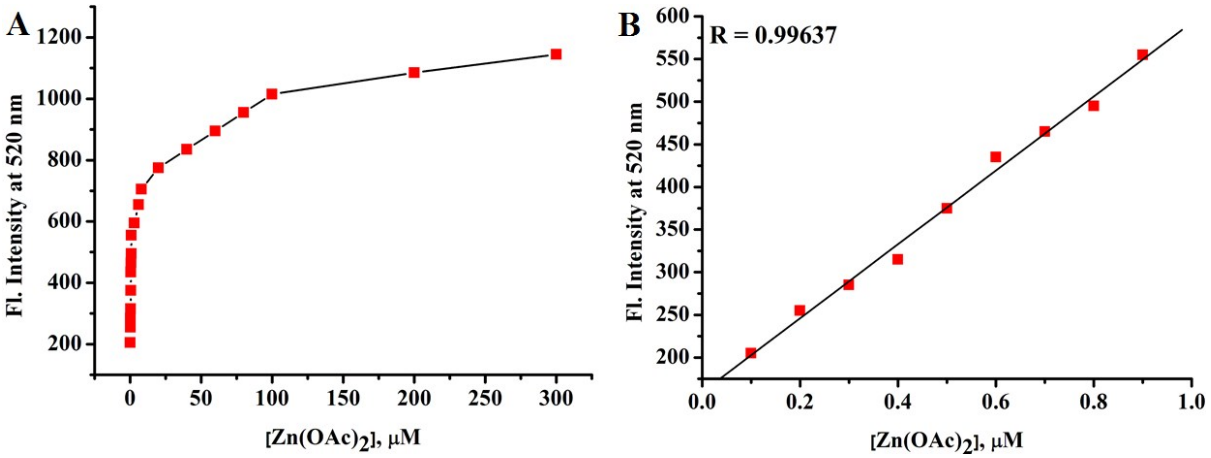

Fig. S30 Emission intensities of **A6** (10 μM, DMSO– water (9 : 1, v/v, 0.1 M HEPES buffer, pH 7.4, λ_{ex}, 337 nm; $\lambda_{em,}$ 520 nm) as a function of added $Zn(OAc)_2$ (0- 300 μM). Linear region of the (right)

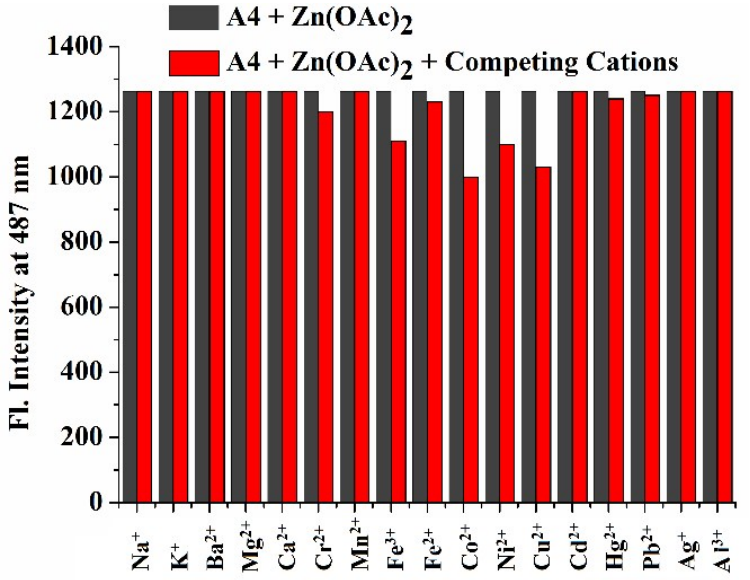

Fig. S31 Effect of common cations on the emission intensities of [A4 + $Zn(OAc)_2$] system (DMSO–water, 9 : 1, v/v, 0.1 M HEPES buffer, pH 7.4, λ_{ex}, 370 nm; λ_{em}, 487 nm)

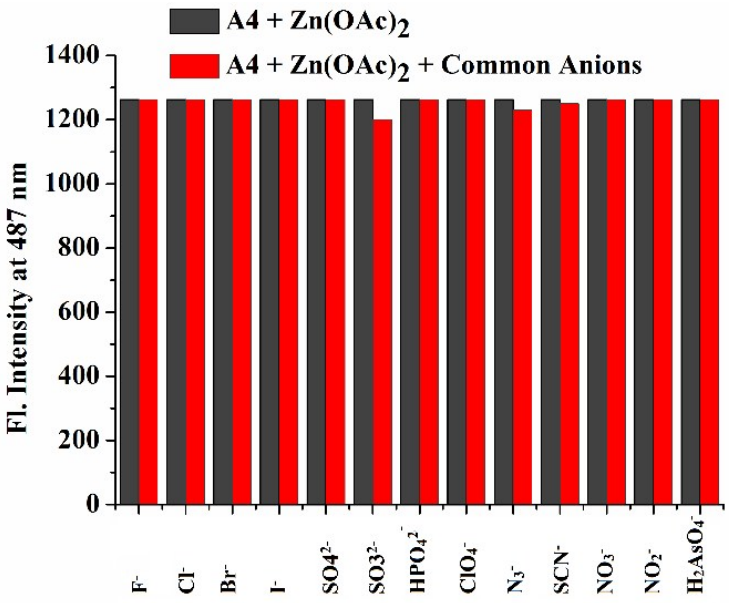

Fig. S32 Effect of common anions on the emission intensities of [A4 + $Zn(OAc)_2$] system (DMSO–water, 9 : 1, v/v, 0.1 M HEPES buffer, pH 7.4, λ_{ex}, 370 nm; λ_{em}, 487 nm)

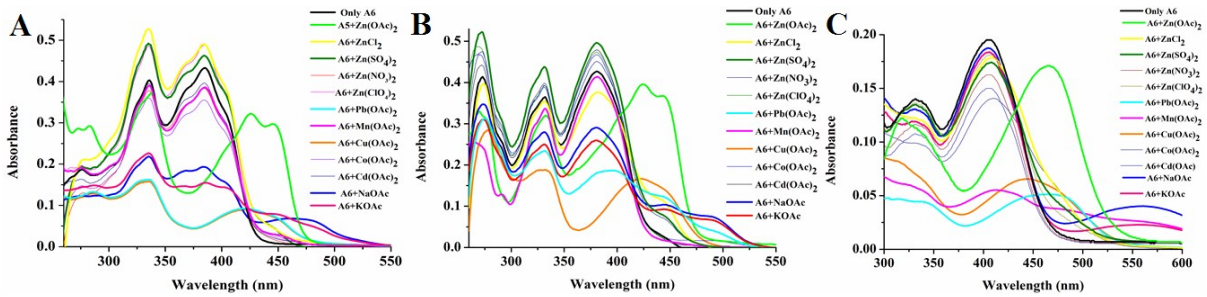

Fig. S33 Effect of equi molar of other salts (including the acetate salts with different metal ions and the zinc salts with different anions) on the absorption spectra of A4, A5 and A6 (left to right).

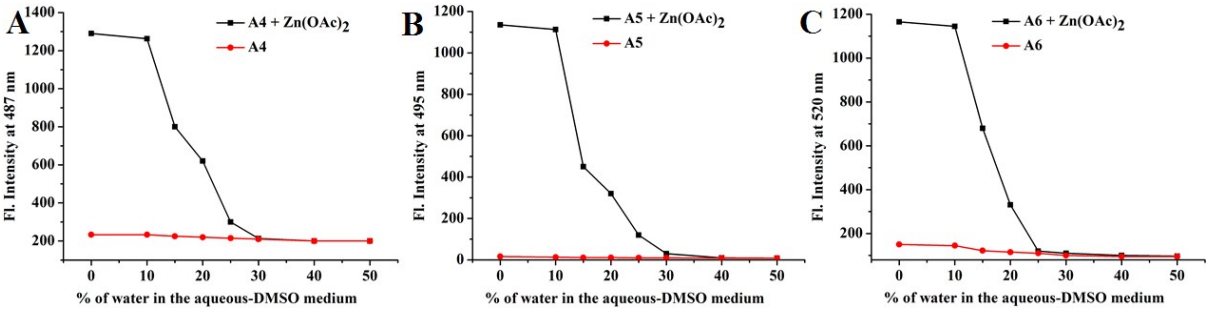

Fig. S34 Effects of increasing water contents of the aqueous-DMSO medium on emission character of A4, A5 and A6 and their ZA adducts (left to right).

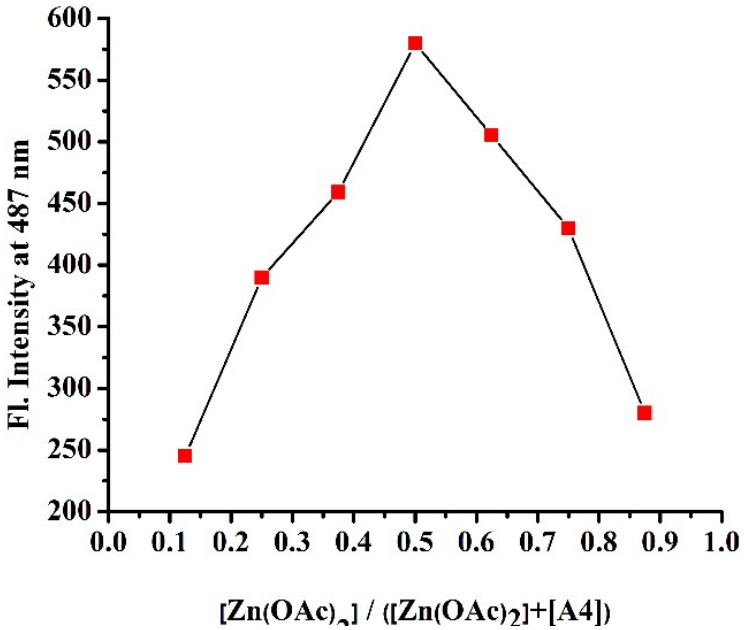

Fig. S35 Job's plot for determination of stoichiometry of the [**A4** + $Zn(OAc)_2$] adduct in DMSO–water, 9 : 1, v/v, 0.1 M HEPES buffer, pH 7.4, λ_{ex}, 370 nm; λ_{em}, 487 nm)

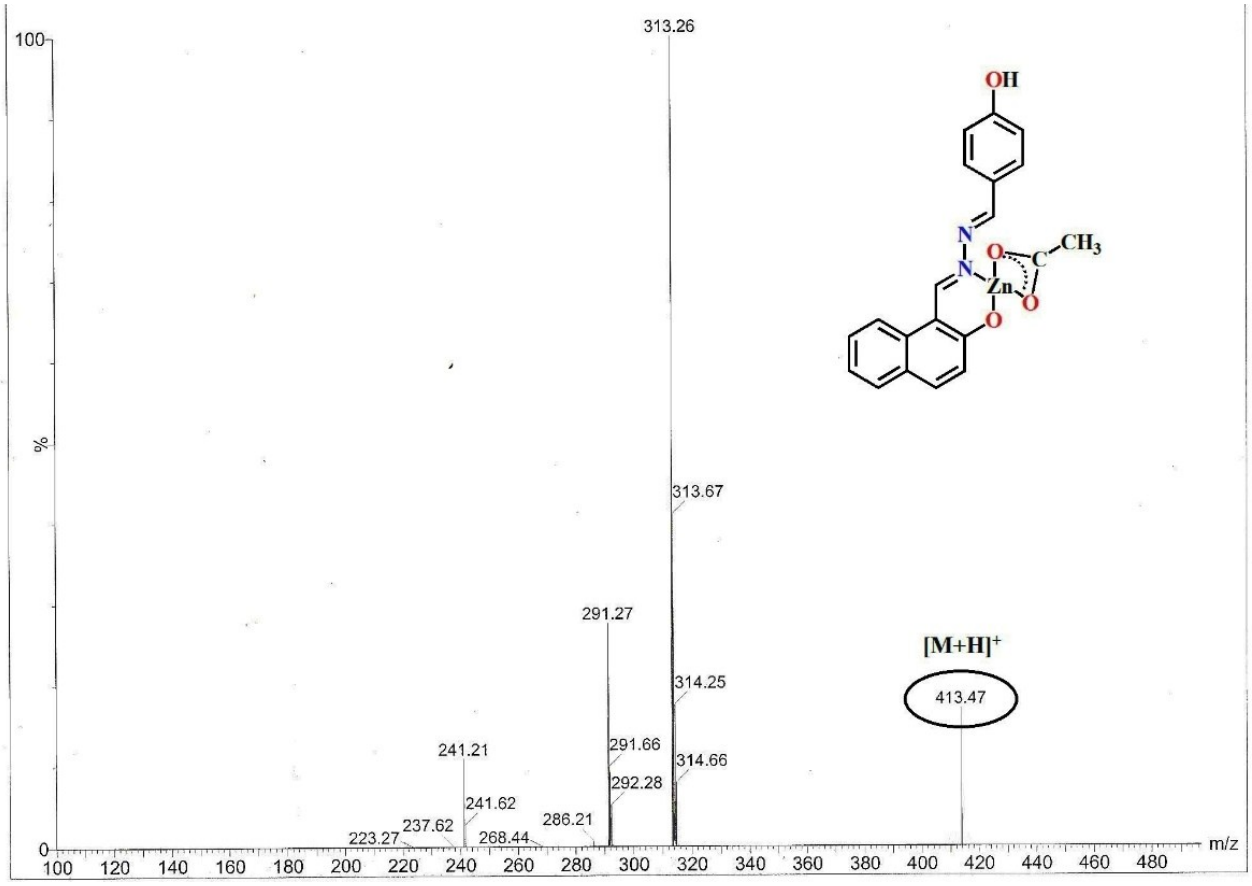

Fig. S36 QTOF-MS(+) spectrum of [A4-$Zn(OAc)_2$] adduct

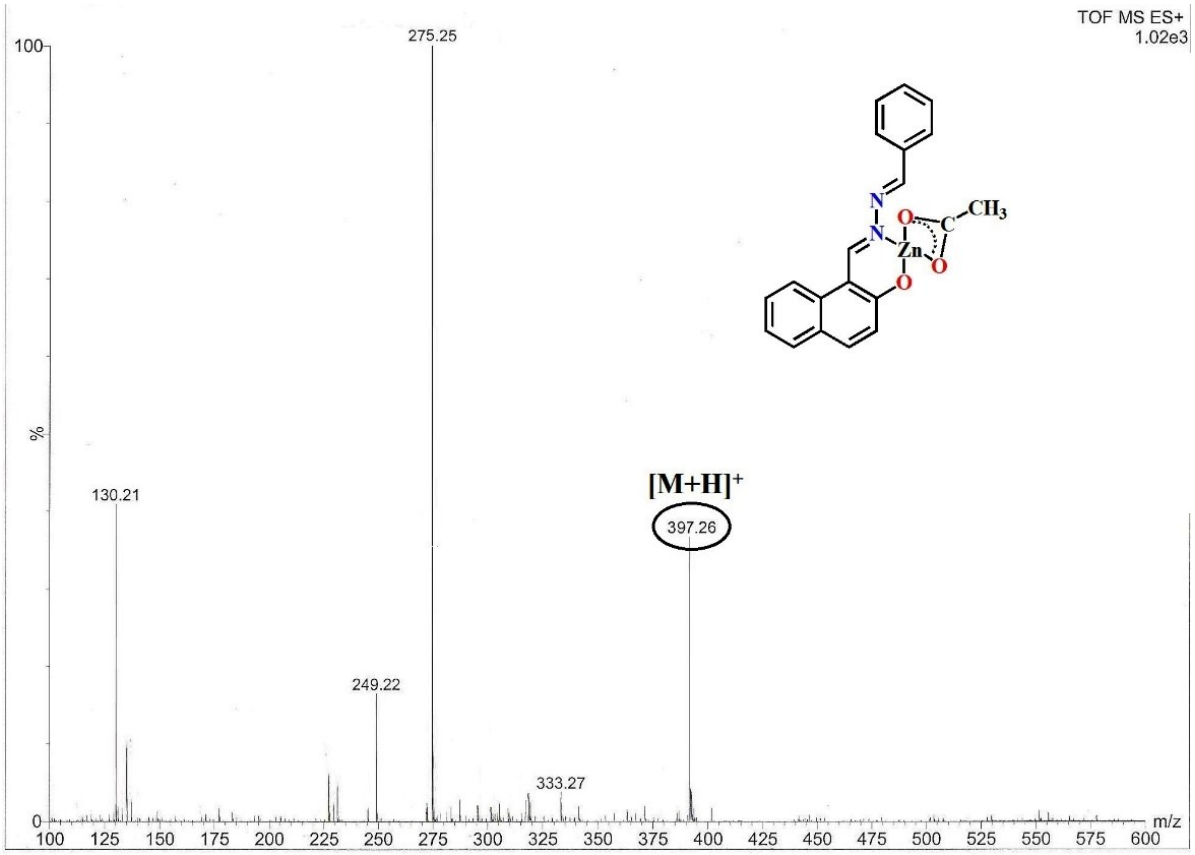

Fig. S37 QTOF-MS(+) spectrum of [A5-Zn(OAc)$_2$] adduct

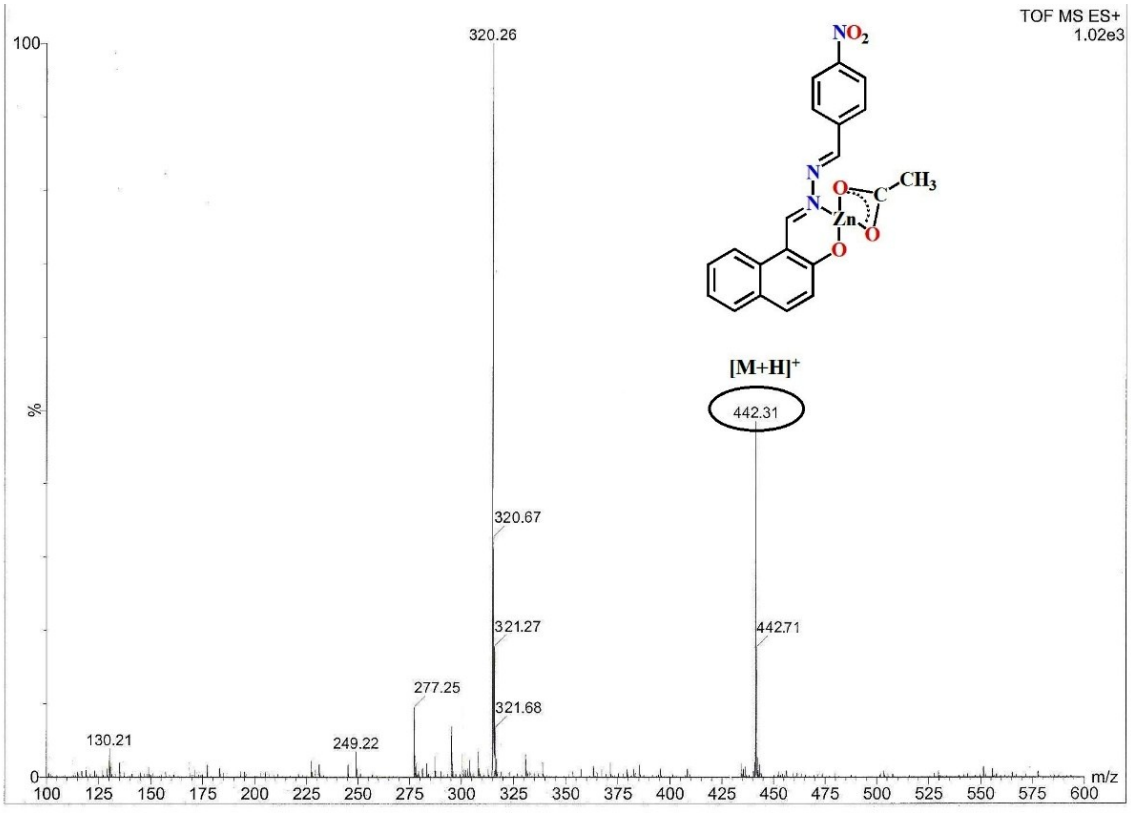

Fig. S38 QTOF-MS(+) spectrum of [A6-Zn(OAc)$_2$] adduct

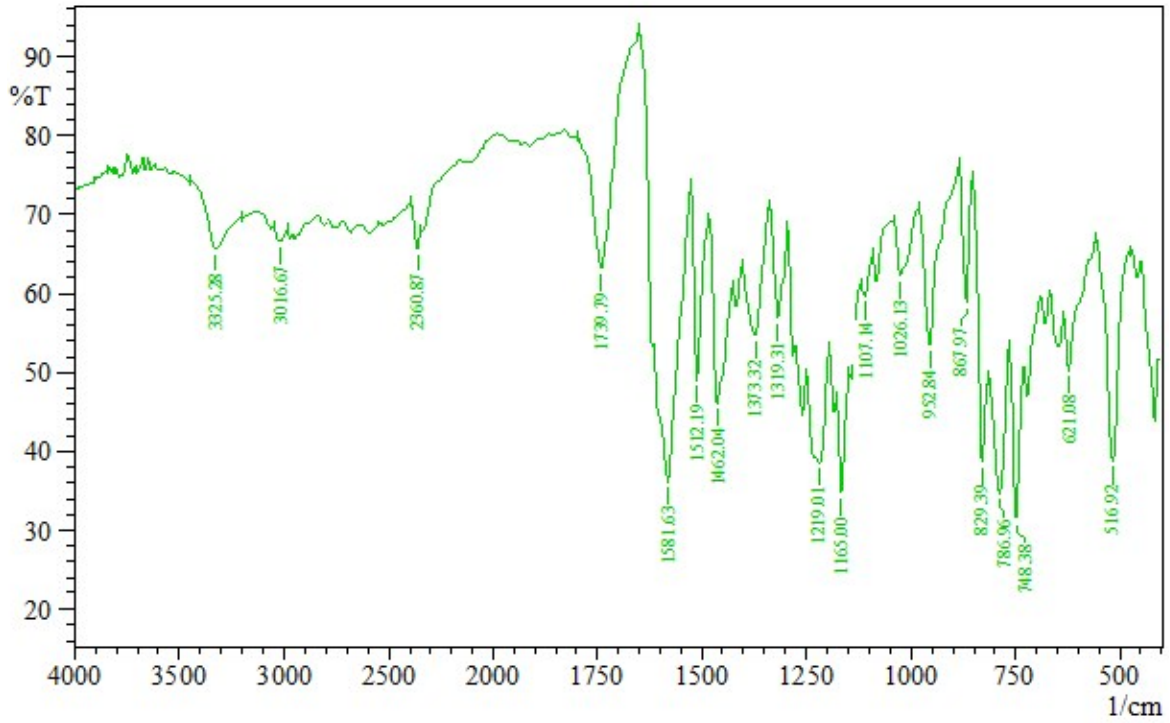

Fig. S39 FTIR spectrum of [A4-Zn(OAc)$_2$] adduct

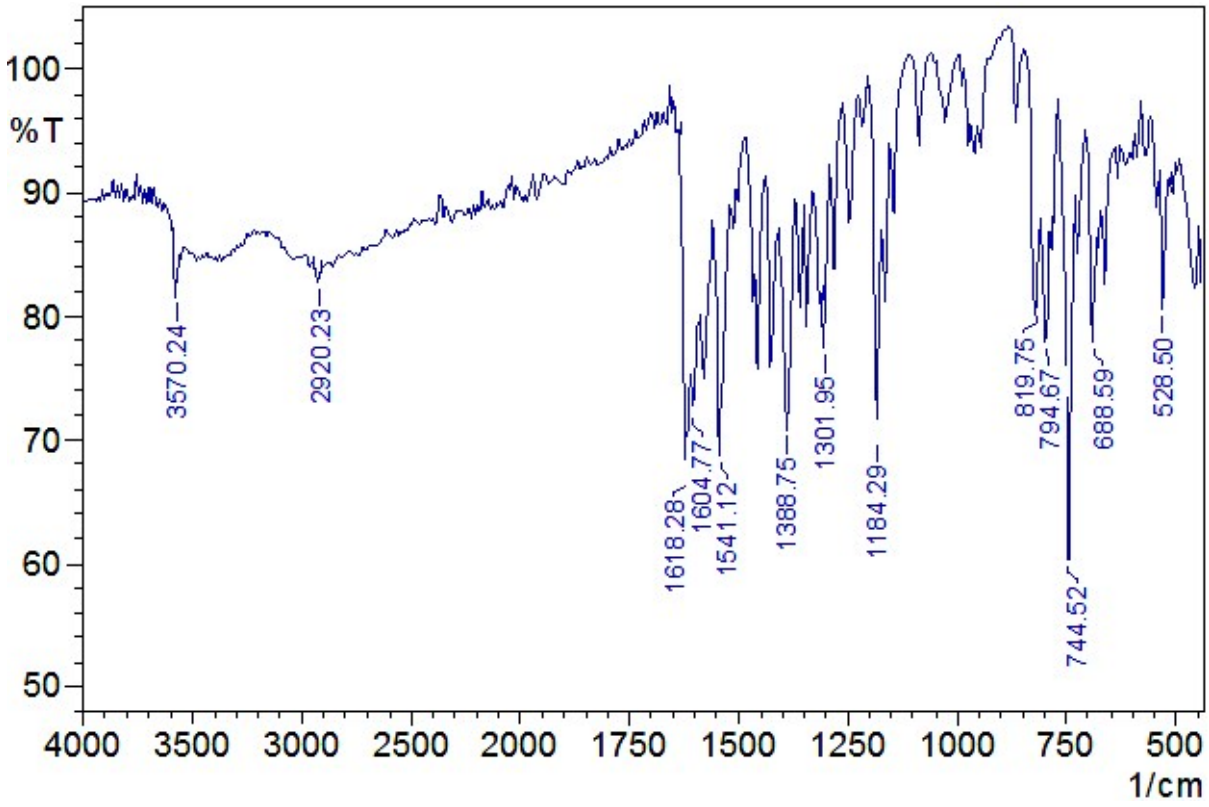

Fig. S40 FTIR spectrum of [A5-Zn(OAc)$_2$] adduct

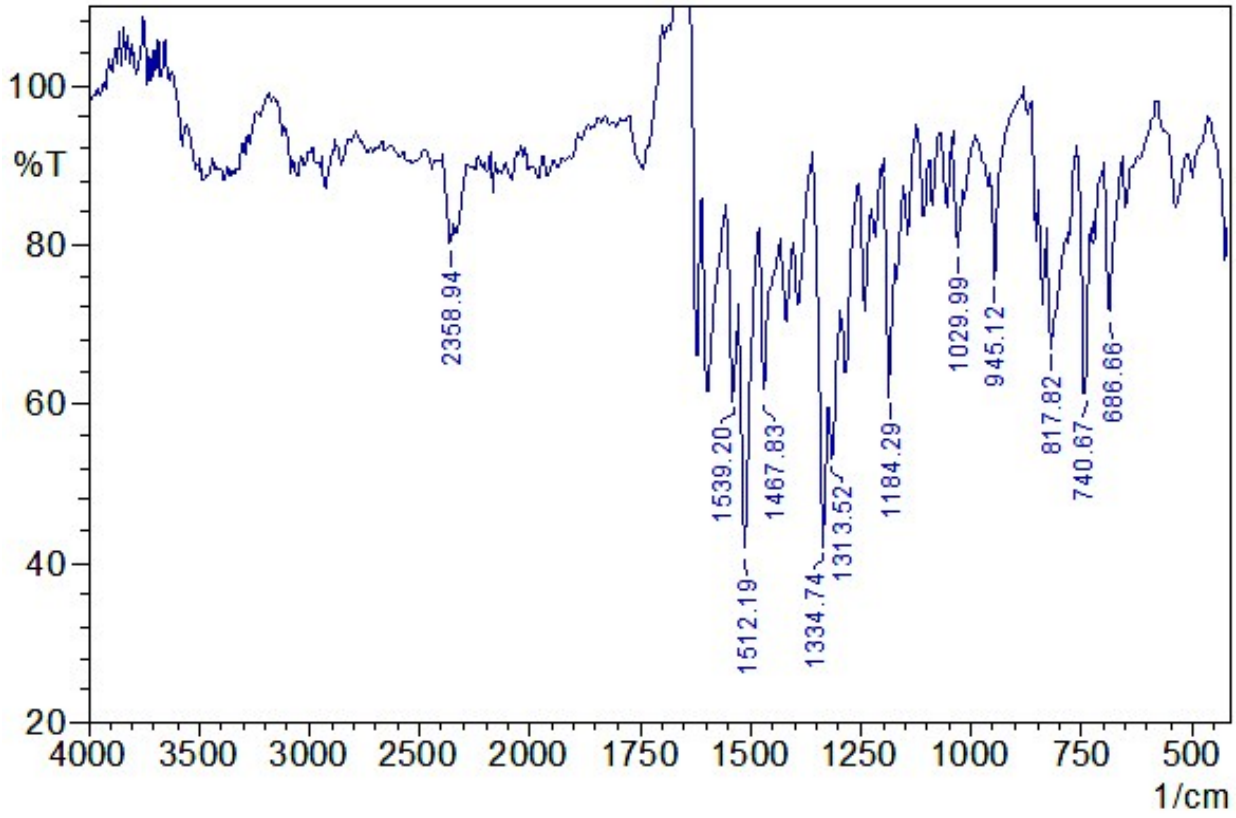

Fig. S41 FTIR spectrum of [A6-$Zn(OAc)_2$] adduct

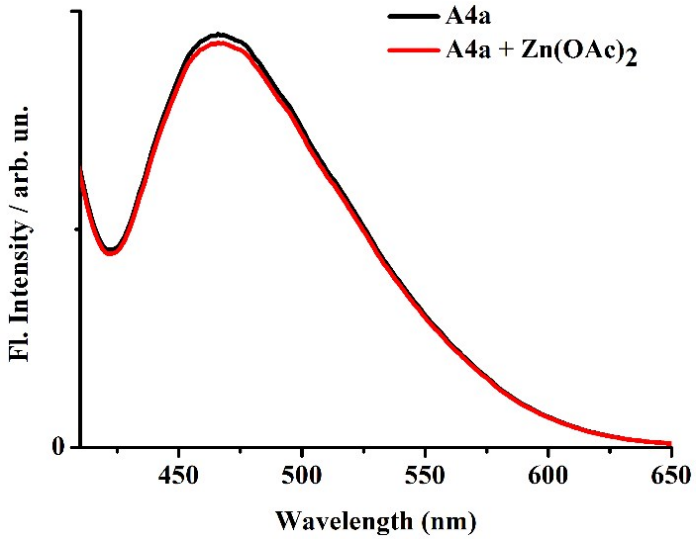

Fig. S42 Effect of $Zn(OAc)_2$ (100 μM) on the emission spectra of A4a (10 μM, λ_{ex}, 355 nm; $\lambda_{em,}$ 465 nm) in water-DMSO (1: 9, v/v).

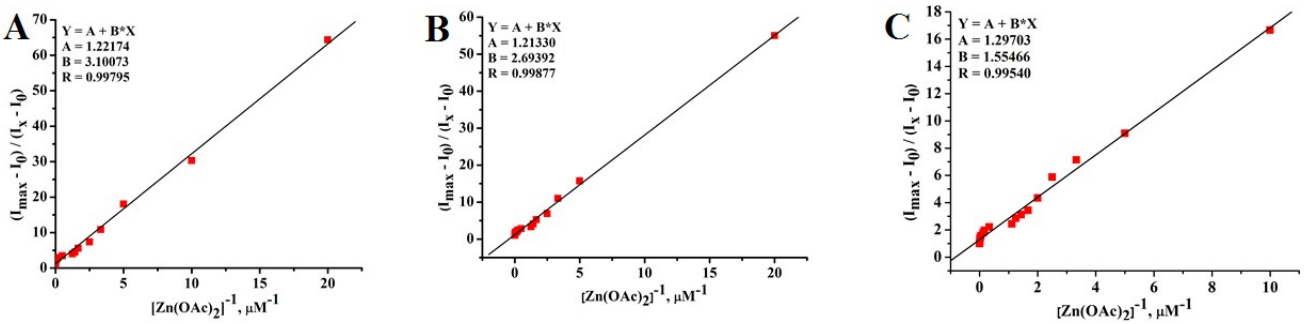

Fig. S43 Determination of binding constant of [A] **A4** (λ_{ex}, 370 nm; λ_{em}, 487 nm, from Fig. 3), [B] A5 (λ_{ex}, 430 nm; λ_{em}, 495 nm, from Fig. S21A) and [C] A6 (λ_{ex}, 337 nm; λ_{em}, 520 nm, from Fig. S21B) for $Zn(OAc)_2$ in DMSO–water = 9 : 1, v/v, 0.1 M HEPES buffer, pH 7.4

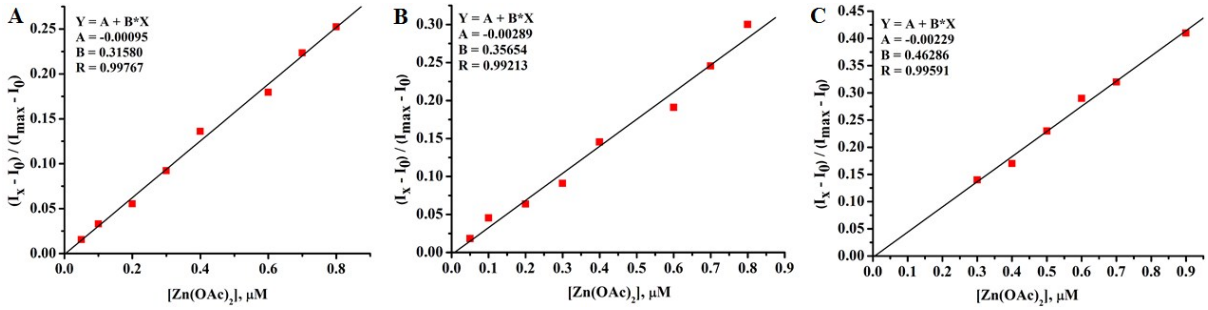

Fig. S44 Emission intensities of [A] **A4** (10 μM, λ_{ex}, 370 nm; λ_{em}, 487 nm, from Fig. 3); [B] **A5** (10 μM, λ_{ex}, 430 nm; λ_{em}, 495 nm from Fig. S21A) and [C] **A6** (10 μM, λ_{ex}, 337 nm; λ_{em}, 520 nm from Fig. S21B) as a function of added $Zn(OAc)_2$ in DMSO– water (9 : 1, v/v), 0.1 M HEPES buffer, pH 7.4

Table S1 Crystal data and structure refinement for A4 and A6

	A4 (CCDC No.: 1018133)	**A6 (CCDC No.: 1415557)**
Empirical formula	$C_{18}H_{14}N_2O_2$	$C_{18}H_{13}N_3O_3$
Formula weight	290.31g/mol	319.31 g/mol
Temperature	296(2) K	296(2) K
Wavelength	0.71073 Å	0.71073 Å
Crystal system	Monoclinic	Triclinic
Space group	*P 1 21/c 1*	P -1
Unit cell dimensions	a = 5.9644(5) Å; α = 90° b = 14.7386(12) Å; β = 92.149(6)° c = 16.5422(13) Å; γ = 90°	a = 7.2028(3) Å; α = 81.753(3)° b = 7.9197(3) Å; β = 84.845(2)° c = 14.7696(6) Å; γ = 65.428(2)°
Volume	1453.2(2) $Å^3$	757.87(5) $Å^3$
Z	4	2
Density (calculated)	1.327 g/cm^3	1.399 g/cm^3
Absorption coefficient	0.088 mm^{-1}	0.098 mm^{-1}
F(000)	608	332
Crystal size	0.16 x 0.10 x 0.04 mm^3	0.18 x 0.14 x 0.04 mm^3
Theta range for data collection	1.85 to 28.42°	3.11 to 26.29°
Index ranges	-7<=h<=7, -17<=k<=19, -21<=l<=22	-8<=h<=8, -9<=k<=9, -18<=l<=18
Reflections collected	26550	11866
Independent reflections	3611 [R(int) = 0.0562]	3048 [R(int) = 0.0331]
Completeness to theta = 22.21°	99.0%	99.4%
Absorption correction	multi-scan	multi-scan
Ratio of min. to max. transmission	0.894	0.923
Refinement method	Full-matrix least-squares on F^2	Full-matrix least-squares on F^2
Refinement program	SHELXL-2014 (Sheldrick, 2014)	SHELXL-2014/6 (Sheldrick, 2014)
Data / restraints / parameters	3611 / 0 / 201	3048 / 0 / 219
Goodness-of-fit on F^2	1.036	1.042
Final R indices [I>2sigma(I)]	R1 = 0.0527, wR2 = 0.1493	R1 = 0.0477, wR2 = 0.1300
R indices (all data)	R1 = 0.1137, wR2 = 0.1925	R1 = 0.0806, wR2 = 0.1547
Largest diff. peak and hole	0.239 and -0.156 $eÅ^{-3}$	0.171 and -0.172 $eÅ^{-3}$
R.M.S. deviation from mean	0.038 $eÅ^{-3}$	0.057 $eÅ^{-3}$

Table S2 Selected bond lengths (Å) for A4

O001-C008	1.358(2)	N002-C00A	1.283(2)
N002-N003	1.387(2)	N003-C007	1.301(2)
O004-C00E	1.312(2)	C005-C00C	1.389(2)
C005-C00D	1.398(2)	C005-C00A	1.443(2)
C006-C00E	1.415(3)	C006-C007	1.421(2)
C006-C009	1.446(2)	C008-C00H	1.385(2)
C008-C00B	1.389(3)	C009-C00G	1.412(3)
C009-C00F	1.418(3)	C00B-C00C	1.376(3)
C00D-C00H	1.364(3)	C00E-C00L	1.417(3)
C00F-C00I	1.368(3)	C00G-C00J	1.410(3)
C00G-C00K	1.420(3)	C00I-C00M	1.385(3)
C00J-C00M	1.354(3)	C00K-C00L	1.348(3)

Table S3 Selected bond angles (°) for A4

C00A-N002-N003	113.80(15)	C007-N003-N002	117.16(15)
C00C-C005-C00D	117.37(17)	C00C-C005-C00A	120.81(16)
C00D-C005-C00A	121.81(16)	C00E-C006-C007	119.24(18)
C00E-C006-C009	119.48(18)	C007-C006-C009	121.27(17)
N003-C007-C006	122.47(17)	O001-C008-C00H	118.31(17)
O001-C008-C00B	122.52(17)	C00H-C008-C00B	119.17(18)
C00G-C009-C00F	117.11(19)	C00G-C009-C006	119.66(18)
C00F-C009-C006	123.15(17)	N002-C00A-C005	122.41(16)
C00C-C00B-C008	119.79(17)	C00B-C00C-C005	121.67(17)
C00H-C00D-C005	121.39(17)	O004-C00E-C006	122.02(18)
O004-C00E-C00L	118.9(2)	C006-C00E-C00L	119.1(2)
C00I-C00F-C009	121.5(2)	C00J-C00G-C009	119.4(2)
C00J-C00G-C00K	122.4(2)	C009-C00G-C00K	118.2(2)
C00D-C00H-C008	120.54(17)	C00F-C00I-C00M	120.8(2)
C00M-C00J-C00G	121.9(2)	C00L-C00K-C00G	122.6(2)
C00K-C00L-C00E	120.9(2)	C00J-C00M-C00I	119.3(2)

Table S4 Selected bond lengths (Å) for A6

O1-C00D	1.3484(19)	O1-H1	0.82
N002-C009	1.2860(18)	N002-N003	1.4037(18)
N003-C007	1.2744(19)	O3-N1	1.227(2)
N1-O2	1.215(2)	N1-C00A	1.472(2)
C007-C00B	1.463(2)	C007-H007	0.93
C008-C00D	1.396(2)	C008-C00C	1.441(2)
C008-C009	1.443(2)	C009-H009	0.93
C00A-C00E	1.373(2)	C00A-C00F	1.376(2)
C00B-C00H	1.385(2)	C00B-C00G	1.392(2)
C00C-C00L	1.412(2)	C00C-C00I	1.422(2)
C00D-C00K	1.413(2)	C00E-C00G	1.376(2)
C00E-H00E	0.93	C00F-C00H	1.386(2)
C00F-H00F	0.93	C00G-H00G	0.93
C00H-H00H	0.93	C00I-C00J	1.413(3)
C00I-C00M	1.413(2)	C00J-C00K	1.357(2)
C00J-H00J	0.93	C00K-H00K	0.93
C00L-C00N	1.357(2)	C00L-H00L	0.93
C00M-C00O	1.346(3)	C00M-H00M	0.93
C00N-C00O	1.398(3)	C00N-H00N	0.93
C00O-H00O	0.93		

Table S5 Selected bond angles (°) for A6

C00D-O1-H1	109.5	C009-N002-N003	113.34(13)
C007-N003-N002	112.90(14)	O2-N1-O3	123.40(16)
O2-N1-C00A	118.52(17)	O3-N1-C00A	118.07(17)
N003-C007-C00B	121.52(15)	N003-C007-H007	119.2
C00B-C007-H007	119.2	C00D-C008-C00C	118.96(14)
C00D-C008-C009	119.80(14)	C00C-C008-C009	121.22(15
N002-C009-C008	121.90(15)	N002-C009-H009	119.0
C008-C009-H009	119.0	C00E-C00A-C00F	122.46(14)
C00E-C00A-N1	119.09(16)	C00F-C00A-N1	118.45(15)
C00H-C00B-C00G	119.21(14)	C00H-C00B-C007	119.87(15)
C00G-C00B-C007	120.91(14)	C00L-C00C-C00I	116.99(15)
C00L-C00C-C008	123.71(14)	C00I-C00C-C008	119.31(16)
O1-C00D-C008	122.78(14)	O1-C00D-C00K	116.35(16)
C008-C00D-C00K	120.87(16)	C00A-C00E-C00G	118.71(15)
C00A-C00E-H00E	120.6	C00G-C00E-H00E	120.6
C00A-C00F-C00H	118.24(15)	C00A-C00F-H00F	120.9
C00H-C00F-H00F	120.9	C00E-C00G-C00B	120.63(15)
C00E-C00G-H00G	119.7	C00B-C00G-H00G	119.7
C00B-C00H-C00F	120.75(16)	C00B-C00H-H00H	119.6
C00F-C00H-H00H	119.6	C00J-C00I-C00M	121.86(16)
C00J-C00I-C00C	118.72(16)	C00M-C00I-C00C	119.42(18)
C00K-C00J-C00I	122.13(16)	C00K-C00J-H00J	118.9
C00I-C00J-H00J	118.9	C00J-C00K-C00D	119.92(18)
C00J-C00K-H00K	120.0	C00D-C00K-H00K	120.0
C00N-C00L-C00C	121.64(17)	C00N-C00L-H00L	119.2
C00C-C00L-H00L	119.2	C00O-C00M-C00I	121.54(18)
C00O-C00M-H00M	119.2	C00I-C00M-H00M	119.2
C00L-C00N-C00O	121.0(2)	C00L-C00N-H00N	119.5
C00O-C00N-H00N	119.5	C00M-C00O-C00N	119.39(19)
C00M-C00O-H00O	120.3	C00N-C00O-H00O	120.3

Table S6 Data from theoretical DFT studies

Compound	Electronic transitions	Energy[a] (eV)	Wavelength (nm)	fb	Transitions involved
A4	S0→S1	3.4686	357.45	0.3989	HOMO→LUMO
	S0→S2	3.5516	349.09	0.0378	HOMO-3→LUMO HOMO-1→LUMO HOMO→LUMO HOMO→LUMO+1
	S0→S3	4.0388	306.98	0.0531	HOMO-3→LUMO HOMO-3→LUMO+1 HOMO-2→LUMO HOMO-1→LUMO HOMO-1→LUMO+1 HOMO→LUMO+1
	S0→S4	4.1420	299.34	0.0389	HOMO-3→LUMO+1 HOMO-1→LUMO+1 HOMO→LUMO+1
	S0→S5	4.1913	295.81	0.1426	HOMO-3→LUMO HOMO-2→LUMO HOMO-2→LUMO+1 HOMO-1→LUMO+1 HOMO-1→LUMO+3 HOMO→LUMO+1 HOMO→LUMO+3
	S0→S6	4.3133	287.45	0.3957	HOMO-3→LUMO HOMO-2→LUMO HOMO-1→LUMO HOMO-1→LUMO+1 HOMO→LUMO+1
	S0→S7	4.6165	268.57	0.0078	HOMO-4→LUMO HOMO-4→LUMO+1 HOMO-2→LUMO+1 HOMO-1→LUMO+2 HOMO→LUMO+2
	S0→S8	4.6258	268.03	0.0113	HOMO-4→LUMO HOMO-3→LUMO+1 HOMO-2→LUMO HOMO-2→LUMO+1 HOMO-1→LUMO+2 HOMO-1→LUMO+3 HOMO-1→LUMO+4 HOMO→LUMO+1 HOMO→LUMO+3
	S0→S9	4.7755	259.63	0.0150	HOMO-5→LUMO HOMO-3→LUMO+1 HOMO-3→LUMO+4 HOMO-2→LUMO HOMO-2→LUMO+1 HOMO-1→LUMO+1 HOMO-1→LUMO+4 HOMO→LUMO+3 HOMO→LUMO+4

	S0→S10	4.9262	251.68	0.0235	HOMO-5→LUMO HOMO-3→LUMO+1 HOMO-1→LUMO+2 HOMO-1→LUMO+4 HOMO→LUMO+2 HOMO→LUMO+4
[A4+Zn(OAc)$_2$] adduct	S0→S1	2.9116	425.83	0.8629	HOMO→LUMO
	S0→S2	3.5555	348.71	0.2180	HOMO-3→LUMO HOMO-2→LUMO HOMO-1→LUMO
	S0→S3	3.6235	342.17	0.0090	HOMO-3→LUMO HOMO-2→LUMO
	S0→S4	3.7677	329.07	0.0387	HOMO-3→LUMO HOMO-2→LUMO HOMO-1→LUMO HOMO →LUMO+1
	S0→S5	3.9833	311.26	0.1518	HOMO-2→LUMO HOMO-1→LUMO HOMO-1 →LUMO+1 HOMO →LUMO+1
	S0→S6	4.3870	282.62	0.0007	HOMO-4→LUMO HOMO-4→LUMO+1 HOMO-1→LUMO+3 HOMO→LUMO+2 HOMO→LUMO+3
	S0→S7	4.4842	276.49	0.0179	HOMO-8→LUMO HOMO-7→LUMO HOMO-6→LUMO HOMO-5→LUMO HOMO-4→LUMO HOMO-3→LUMO+1 HOMO→LUMO+2 HOMO→LUMO+3
	S0→S8	4.5274	273.85	0.0271	HOMO-8→LUMO HOMO-7→LUMO HOMO-6→LUMO HOMO-3→LUMO+1 HOMO-1→LUMO+1 HOMO→LUMO+2
	S0→S9	4.5886	270.20	0.0128	HOMO-6→LUMO HOMO-5→LUMO HOMO-2→LUMO+1 HOMO-1→LUMO+1 HOMO→LUMO+2 HOMO→LUMO+5
	S0→S10	4.6205	268.33	0.0527	HOMO-5→LUMO HOMO-2→LUMO+1 HOMO-1→LUMO+1 HOMO→LUMO+5

Table. S7 Data from theoretical DFT studies

Compound	Electronic transitions	Energy[a] (eV)	Wavelength (nm)	f[b]	Transitions involved
A5	S0→S1	3.2113	386.09	0.8786	HOMO→LUMO
	S0→S2	3.3056	375.08	0.0086	HOMO-1→LUMO
	S0→S3	3.9115	316.98	0.1485	HOMO-3→LUMO HOMO-2→LUMO HOMO→LUMO+2
	S0→S4	4.0179	308.58	0.0660	HOMO-3→LUMO HOMO→LUMO+1
	S0→S5	4.2031	294.98	0.2517	HOMO-3→LUMO HOMO-2→LUMO HOMO→LUMO+1
	S0→S6	4.3961	282.03	0.0195	HOMO-4→LUMO HOMO-4→LUMO+1 HOMO→LUMO+3
	S0→S7	4.4105	281.11	0.0051	HOMO-1→LUMO+1 HOMO-1→LUMO+4
	S0→S8	4.6512	266.57	0.0509	HOMO-3→LUMO+1 HOMO-2→LUMO HOMO-2→LUMO+1 HOMO→LUMO+1 HOMO→LUMO+2
	S0→S9	4.8546	255.40	0.0184	HOMO-5→LUMO HOMO-3→LUMO+1 HOMO→LUMO+3 HOMO→LUMO+4
	S0→S10	5.0162	247.17	0.0406	HOMO-5→LUMO HOMO-4→LUMO HOMO-4→LUMO+1 HOMO→LUMO+3 HOMO→LUMO+4
[A5+Zn(OAc)$_2$] adduct	S0→S1	2.9182	424.87	0.7528	HOMO→LUMO
	S0→S2	3.5439	349.85	0.1942	HOMO-1→LUMO HOMO→LUMO+5
	S0→S3	3.6413	340.50	0.0095	HOMO-3→LUMO
	S0→S4	3.8660	320.70	0.0165	HOMO-2→LUMO HOMO→LUMO+1
	S0→S5	4.0251	308.03	0.3094	HOMO-2→LUMO HOMO→LUMO+1
	S0→S6	4.2389	292.49	0.0180	HOMO-4→LUMO HOMO-4→LUMO+1 HOMO-2→LUMO+3 HOMO→LUMO+3
	S0→S7	4.3968	281.99	0.0247	HOMO-8→LUMO

					HOMO-7→LUMO HOMO-6→LUMO HOMO-3→LUMO+1 HOMO→LUMO+2
	S0→S8	4.4338	279.63	0.0173	HOMO-8→LUMO HOMO-7→LUMO HOMO-6→LUMO HOMO-3→LUMO+1 HOMO→LUMO+2
	S0→S9	4.5599	271.90	0.0291	HOMO-1→LUMO+1 HOMO→LUMO+5
	S0→S10	4.6301	267.78	0.0002	HOMO-5→LUMO

Table. S8 Data from theoretical DFT studies

Compound	**Electronic transitions**	**Energy[a] (eV)**	**Wavelength (nm)**	**f[b]**	**Transitions involved**
A6	S0→S1	2.4445	507.19	0.0293	HOMO→LUMO
	S0→S2	3.0745	403.27	0.4085	HOMO-3→LUMO HOMO-2→LUMO HOMO-1→LUMO
	S0→S3	3.1656	391.66	0.0028	HOMO-2→LUMO HOMO-1→LUMO
	S0→S4	3.4785	356.43	0.2365	HOMO-6→LUMO HOMO-3→LUMO HOMO-2→LUMO HOMO-1→LUMO HOMO→LUMO+1
	S0→S5	3.4819	356.08	0.0321	HOMO-6→LUMO HOMO-6→LUMO+1 HOMO-6→LUMO+2 HOMO-3→LUMO
	S0→S6	3.6891	336.08	0.1204	HOMO-3→LUMO HOMO-1→LUMO HOMO→LUMO+1
	S0→S7	3.8360	323.21	0.0254	HOMO-4→LUMO
	S0→S8	4.0028	309.74	0.0125	HOMO-10→LUMO HOMO-2→LUMO+1 HOMO-1→LUMO+1 HOMO-1→LUMO+5
	S0→S9	4.0407	306.84	0.0008	HOMO-10→LUMO HOMO-10→LUMO+1 HOMO-10→LUMO+2 HOMO-1→LUMO+1
	S0→S10	4.1599	298.05	0.0275	HOMO-1→LUMO+2 HOMO→LUMO+2
[A6+Zn(OAc)$_2$] adduct	S0→S1	2.0833	595.13	0.4522	HOMO→LUMO

	S0→S2	2.7430	452.01	0.0871	HOMO-1→LUMO
	S0→S3	3.0788	402.70	0.3080	HOMO-2→LUMO HOMO→LUMO+1
	S0→S4	3.1126	398.33	0.1235	HOMO-3→LUMO HOMO-2→LUMO HOMO-2→LUMO+1 HOMO→LUMO+1
	S0→S5	3.2620	380.08	0.0000	HOMO-9→LUMO HOMO-9→LUMO+1
	S0→S6	3.4058	364.03	0.2530	HOMO-3→LUMO HOMO-2→LUMO HOMO→LUMO+1
	S0→S7	3.5835	345.98	0.0308	HOMO-5→LUMO
	S0→S8	3.6584	338.90	0.1301	HOMO-1→LUMO+1
	S0→S9	3.7569	330.02	0.0052	HOMO-12→LUMO HOMO-4→LUMO
	S0→S10	3.7695	328.91	0.0006	HOMO-13→LUMO HOMO-12→LUMO HOMO-12→LUMO+1 HOMO-4→LUMO HOMO-2→LUMO+1